The University of Manitoba

DECOMPOSITION OF METHYL IODIDE IN NITROGEN USING A NEGATIVE CORONA DISCHARGE

by

PHILIP C. HARRIS

A Thesis submitted to the Faculty of Graduate Studies in partial fulfillment of the requirements for the Degree of Master of Science through the Department of Chemistry.

The research work was conducted at the Research Chemistry Branch, Whiteshell Nuclear Research Establishment, Pinawa, Manitoba ROE 1LO.

Winnipeg, Manitoba, 1985

DECOMPOSITION OF METHYL IODIDE IN NITROGREN USING A NEGATIVE CORONA DISCHARGE

BY

PHILIP C. HARRIS

A thesis submitted to the Faculty of Graduate Studies of the University of Manitoba in partial fulfillment of the requirements of the degree of

MASTER OF SCIENCE

I hereby declare that I am the sole author of this thesis.

I authorize the University of Manitoba to lend this thesis to other institutions or individuals for the purpose of scholarly research.

P.C. Harris

I further authorize the University of Manitoba to reproduce this thesis by photocopying or by other means, in total or in part, at the request of other institutions or individuals for the purpose of scholarly research.

P.C. Harris

ACKNOWLEDGEMENTS

Dr. D.F. Torgerson - for providing me with the benefits of his guidance and enthusiasm throughout the duration of my Master's.

Dr. L.W. Dickson - with whom I had many illuminating discussions, and for always answering his phone.

A. Toft-Hall - who showed infinite patience (sometimes) in putting up with me in the laboratory.

B.C. Skinner and R.J. Jerrard - for their advice on computational and numerical analysis, and for many enjoyable hands of lunchtime bridge.

P. McCooeye - for her perseverance in typing, editing and revising this manuscript.

Dr. D.J. Wren - for always being able to suggest a solution (or several solutions) to a problem.

Building 300 Machine Shop and Electrical Shop - without whose aid this work would never have been completed.

Also, a heartfelt thank you to the numerous friends and associates who gave me their advice, support and/or guidance throughout the course of this project.

DEDICATION

To my Mother, for standing beside me when I needed support, and for getting behind me when I needed a push.

ABSTRACT

The decomposition of methyl iodide transported through a coaxial cylinder corona discharge in a nitrogen carrier gas has been investigated experimentally and theoretically. Experiments were carried out at room temperature and atmospheric pressure. The gas flow rates ranged from 0.5 to 2.5 L/min, the initial concentration of methyl iodide was varied from 10 to 500 μL/L, and the discharge current was varied from 0 to ∿ 3 mA.

In developing a mathematical model to explain the data, attention has been paid first to deriving an expression which accurately describes the electric field in the discharge tube, and subsequently to developing an equation which predicts the rate of electron capture by methyl iodide under conditions of a broad electron energy distribution.

A reaction mechanism has been determined which shows excellent agreement with the experimental data for methyl iodide decomposition. On the basis of this mechanism, the electron attachment cross section at the resonance energy has been determined to be 186 ± 20 Å^2, and the rate constant of the reaction

$$CH_3 + CH_3I \rightarrow C_2H_6 + I$$

has been found to be $(2.0 \pm 0.3) \times 10^{-14}$ cm^{3}molecule^{-1}s^{-1} at 300 K and 760 torr.

TABLE OF CONTENTS

INTRODUCTION

The interaction of low energy electrons ($\leq$ 15 ev) with atoms and molecules is of interest to the fields of physics, chemistry, biology and engineering[1]. The production of negative ions by electron capture and their subsequent reaction is a subject of considerable theoretical and practical importance. Besides providing information on molecular structure and bonding[2], knowledge of the interaction between electrons and matter has applications in atmospheric chemistry[3,4], polymer formation[5], gas lasers[6], and the biological sciences[7].

The basic physics and chemistry of the interaction of electrons with molecules has been studied through a variety of experimental techniques, such as swarm methods[8,9], electron beams[10] and swarm beam techniques[11]. These methods have provided a wealth of valuable information on electron attachment rates and cross sections for various atoms and molecules.

In order to use low energy electrons in industrial applications, a convenient source of free electrons is required. Although there are several conceivable methods to produce these free electrons, the simplest procedure is to use a low power discharge[12]. Corona discharges can be readily developed in gases using a variety of discharge geometries, including a thin wire coaxially aligned with a hollow grounded cylinder. The discharge thus formed may produce numerous reactive species, which then initiate a complicated series of chemical reactions[13].

Corona discharges have frequently been used as electrostatic precipitators, and may be employed to destroy bacteria[14] and toxic chemical pollutants[15]. It has been suggested[12] that a corona discharge may also provide an efficient method for the destruction of organic iodides, and thus have applications in the ventilation systems of nuclear reactors and nuclear fuel reprocessing plants.

In coaxial cylinder discharge tubes, a large negative potential applied to the filament of the discharge tube results in the primary charge carriers being electrons and negative ions. This provides a strongly reducing medium, which has previously been used to promote the decomposition of organic iodides in RI/air gas streams[16,17]. However, due to the apparent complexity of the reaction mechanism, no detailed kinetic model has yet been developed which explains the rate of organic iodide decomposition in these systems.

In an effort to elucidate some aspects of this process, the decomposition of methyl iodide in a corona discharge has been studied, using nitrogen as the carrier gas. Nitrogen was chosen as the carrier gas as it is unreactive towards organic iodides, and yet will provide electron energy characteristics similar to those exhibited by a corona discharge in air. Thus, the interaction of electrons and methyl iodide may be studied in a situation where reactions between the methyl iodide and the carrier gas are relatively unimportant.

An effort was made to understand and explain the observed decomposition of methyl iodide in terms of fundamental physical

parameters (such as the electron capture cross section) and some simple chemical reactions.

THEORY

In order to rationalize the effects of a corona discharge on nitrogen/methyl iodide gas mixtures, an understanding of the fundamental processes in negative discharges at atmospheric pressure is required. Although negative corona discharges are, in general, not well understood[18], the underlying processes governing the development of the discharge are reasonably well known. Physical phenomena which are typically of interest are the growth of current (ionization phenomena), electrostatic parameters (charge density, electric scalar potential, etc.) and electron-ion energy distribution functions. These phenomena are all related to the electric field and thus to the potential difference between the electrodes.

In this work, a coaxial cylinder discharge tube was employed, and operated under conditions where the inner cylinder (a 6.35×10^{-3} cm radius tungsten wire) was maintained at a large negative potential. At voltages greater than the onset voltage, a glow is observed in a cylindrical region of approximately 0.2 cm radius[12] around the central filament. This region will hereafter be referred to as the ionization region or ionization sheath, and it is here that ionizing interactions between electrons and molecules occur. Outside of the ionization sheath, the principal electron-molecule interactions of interest will be attachment reactions. This region is typically referred to as the drift region.

A corona discharge occurs when the discharge geometry gives rise to a very inhomogeneous electric field, such as that which occurs between a co-axial wire and cylinder[19]. The development of a corona discharge is determined by the voltage drop across the electrodes. As the voltage on the stressed electrode (electrode of smaller radius of curvature) is increased, relatively little discharge current will be observed until the onset voltage, V_c, is reached[20]. The small current observed for $V < V_c$ is known as the saturation current[21], and is typically on the order of 10^{-14} to 10^{-11} A[18,21]. This saturation current is due to natural ionization of the gas by cosmic rays and/or the decay of naturally occurring radioisotopes.

The corona discharge is initiated at the threshold (onset) voltage, as evidenced by the dramatic rise in current to a value on the order of 10^{-6} A[22]. The onset of the discharge requires an "avalanche", which is initiated by a free electron[18]. This avalanche may be understood in terms of the following simple mechanism.

A free electron is formed near the stressed electrode due to cosmic rays or other background radiation. The electron is accelerated by the electric field to a sufficient kinetic energy to be capable of ionizing a gas molecule. Ionization occurs, and there are now two free electrons and a positive ion. The positive ion is accelerated to the negative electrode, where it may liberate further electrons or a photon capable of ionizing the gas[23]. Meanwhile, the two electrons are accelerated in the electric field, and may produce further ionization through collisions with the gas molecules.

In order for the discharge to exhibit steady state behaviour, the rate at which ions are lost (due to contact at surfaces) must be compensated for by the rate of ionization. The Townsend criterion[24] for a self-sustaining corona discharge may be written as:

$$\gamma[\exp(\int_{\ell}(\alpha-\eta)d\ell)-1] = 1,$$

where

α is Townsend's primary ionization coefficient and is related to the probability of ionization of the gas by electrons,

γ is the secondary ionization coefficient accounting for cathodic and photochemical processes, and

η is the electron "disappearance" coefficient accounting for the rate of loss of electrons.

Parameters such as α and η are found to be functions of the electric field[25], and thus in non-uniform fields are a function of the discharge geometry. The integral over ℓ determines the region in which these phenomena take place. This leads to complications when one is trying to model a corona discharge, as reaction rates are dependent on the discharge geometry (i.e. the rate of a reaction in the ionization sheath may be significantly different from the rate in the drift region). This is predominantly due to the different electron energies in these regions.

The nature of the interaction between electrons and gas molecules is dependent on the electron energy[19]. The energy of an electron is related to the type of collisions it undergoes and the

acceleration due to the electric field that it experiences between collisions with gas molecules. Thus, in order to determine the electron energy distribution function (eedf), the electric field and the type of collison processes must be known.

Electric Field in the Presence of a Space Charge

An accurate approximation of the electric field may be determined by considering the steady state behaviour of the discharge outside of the ionization region[26]. In this region of lower electric field, the electric scalar potential must satisfy Poisson's equation:

$$\nabla^2 U = -\rho/\varepsilon \qquad (1)$$

where U is the electric potential, ρ is the space charge density, and ε is the dielectric permittivity of the gas.

The electric field:

$$\bar{\chi} = -\nabla U \qquad (2)$$

is used to determine the current density:

$$\bar{J} = \rho \langle k \rangle \bar{\chi} \qquad (3)$$

where $\langle k \rangle$ is the mean ionic mobility.

Conservation of charge requires that:

$$\nabla \cdot \bar{J} = \frac{\partial \rho}{\partial t} \tag{4}$$

which at steady state gives:

$$\nabla \cdot \bar{J} = 0 \quad . \tag{5}$$

Equations 1 to 5 may be combined to give:

$$\nabla \cdot (\varepsilon \nabla^2 U \langle k \rangle \nabla U) = 0 \quad . \tag{6}$$

In principle, solutions to Eqn 6 exist for all discharge geometries. However, analytical solutions may be obtained only for the simplest systems.

The co-axial cylinder discharge is an example of a discharge geometry for which an analytical solution to Eqn 6 exists. This system has been investigated by various authors[27-29], usually under conditions of low current[27,28]. However, the solutions generated previously required the use of approximations which were not valid for the experimental conditions encountered in this work. For this reason, the solution to Eqn 6 will be given in detail.

By symmetry arguments, it is apparent that the electric potential may be expressed (in cylindrical polar coordinates) as being only a function of r, the radial coordinate. Thus, from Eqn 6, we have that:

$$\bar{r} \cdot \varepsilon \nabla^2 U \langle k \rangle \nabla U = \text{constant} \quad . \tag{7}$$

The constant in Eqn 7 may be evaluated easily since $\varepsilon \nabla^2 U \langle k \rangle \nabla U \cdot \bar{r} = \bar{r} \cdot \bar{J}$. At the filament, $|\bar{r}| = a$ and the current density must be $|\bar{J}| = i/2\pi a$ where i is the current per unit length of filament, and a is the radius of the filament. Thus:

$$\bar{r} \cdot \bar{J} = \bar{r} \cdot \varepsilon \nabla^2 U \langle k \rangle \nabla U = \frac{i}{2\pi} \quad . \tag{8}$$

Writing $\nabla U = -\bar{\chi}$, $\nabla^2 U = -\nabla \cdot \bar{\chi}$, and $\bar{\chi} = \chi \hat{r}$, where $\hat{r}$ is a unit vector in the radial direction, we may express Eqn 8 as:

$$r\chi \frac{1}{r} \frac{d}{dr} (r\chi) = \frac{i}{2\pi\varepsilon\langle k \rangle} \tag{9}$$

or:

$$(r\chi) \frac{d}{dr} (r\chi) = \frac{i}{2\pi\varepsilon\langle k \rangle} r \quad . \tag{10}$$

Integration of Eqn 10 from a to r yields:

$$(r\chi)^2 - (a\chi_o)^2 = \frac{i}{2\pi\varepsilon\langle k \rangle} (r^2 - a^2) \tag{11}$$

where χ_o is the electric field at the filament (r=a).

By simple algebra:

$$\chi = \left(\frac{i}{2\pi\varepsilon\langle k \rangle} + \frac{a^2}{r^2} \left(\chi_o^2 - \frac{i}{2\pi\varepsilon\langle k \rangle} \right) \right)^{1/2} \quad . \tag{12}$$

When the applied voltage is less than the onset voltage, the current (and therefore the space charge density) will be zero, and the field for $V < V_c$ may be determined by solving Laplace's equation $\nabla^2 U = 0$. This gives:

$$\chi_{V<V_c} = \frac{V}{r\ln(R/a)} \tag{13}$$

where R is the radius of the discharge tube. In the limit as the applied voltage approaches V_c from the negative side, the current will remain equal to zero, and Eqn 13 must approach Eqn 12:

$$\lim_{V \to V_c} \frac{V}{r\ln(R/a)} = \left(\frac{a^2}{r^2} \chi_o^2 \right)^{1/2} .$$

Obviously, $\chi_o = V_c/a\ln(R/a)$, and Eqn 12 may be written as:

$$\chi(r) = \left(\frac{i}{2\pi\epsilon\langle k \rangle} + \frac{a^2}{r^2} \left(\left(\frac{V_c}{a\ln(R/a)} \right)^2 - \frac{i}{2\pi\epsilon\langle k \rangle} \right) \right)^{1/2} . \tag{14}$$

This form has the same behaviour as that observed experimentally[30] for regions near the filament and near the wall.

At this point, it is useful to consider the relative magnitudes of the terms $(V_c/a\ln(R/a))^2$ and $i/2\pi\epsilon\langle k \rangle$. The value of $i/2\pi\epsilon\langle k \rangle$ will be maximized for conditions where the mean mobility of the ions (assuming constant current) is small. Thus, if we assume that most of

the negative current is carried by I^- ions, we may approximate the average value of the ionic mobility by the mobility of I^- in nitrogen.

Although no values of the mobility of I^- in N_2 exist in the literature, the mobility in Ar is known[31] to be 2.28 ± 0.07 $cm^2V^{-1}s^{-1}$, which is comparable to the mobility in Ar of the isoelectronic ion[32], Cs^+ ($K \simeq 2.10$ $cm^2V^{-1}s^{-1}$). Thus, it will be assumed that the mobility of I^- in nitrogen is the same as that of Cs^+ in nitrogen ($K \simeq 2.30$ $cm^2V^{-1}s^{-1}$)[33]. The use of this value will provide an upper bound on the effect of the space charge, since the mean ionic mobility of the ions present is surely greater than that of I^-. The upper bound on the term $i/2\pi\varepsilon\langle k\rangle$ is $I_T \cdot 1.7 \times 10^7$ $V^2cm^{-2}mA^{-1}$, where I_T is the total discharge current in mA (0.0 mA $\leq I_T \leq 3$ mA for the experimental conditions in this work). Thus, it may be presumed that

$$\frac{i}{2\pi\varepsilon\langle k\rangle} \leq I_T(1.7 \times 10^7 \ V^2cm^{-2}mA^{-1}) \quad . \tag{15}$$

The onset voltage for the discharge is typically found to be on the order of 5×10^3 volts in this work, and thus the term $(V_c/a\ln(R/a))^2$ will be on the order of 10^{10} V^2cm^{-2}. It becomes apparent that:

$$\left(\frac{V_c}{a\ln(R/a)}\right)^2 \gg \frac{i}{2\pi\varepsilon\langle k\rangle} \quad , \tag{16}$$

and that Eqn 14 may be expressed as:

$$\chi(r) = \left(\frac{i}{2\pi\epsilon\langle k\rangle} + \left(\frac{V_c}{r\ln(R/a)}\right)^2\right)^{1/2} \quad . \tag{17}$$

The term $i/2\pi\epsilon\langle k\rangle$ may be determined as a function of the parameters V, V_c, a and R by integrating Eqn 17 over the radius. Since this integral corresponds to $\int_r \bar{\chi}\cdot d\bar{r}$, it is apparent that it must be equal to the potential difference, V. Thus,

$$V = \int_a^R \left(\frac{i}{2\pi\epsilon\langle k\rangle} + \left(\frac{V_c}{r\ln(R/a)}\right)^2\right)^{1/2} dr$$

$$= \sqrt{CR^2+B^2} - \sqrt{Ca^2+B^2} - B\ln\left|\left(\frac{a}{r}\right)\frac{B+\sqrt{CR^2+B^2}}{B+\sqrt{Ca^2+B^2}}\right| \quad , \tag{18}$$

where $C = i/2\pi\epsilon\langle k\rangle$ and $B = V_c/\ln(R/a)$.

Using Eqn 16, we may express Eqn 18 as:

$$V = \sqrt{CR^2+B^2} - B - B\ln\left|\left(\frac{a}{R}\right)\frac{B+\sqrt{CR^2+B^2}}{2B}\right| \quad . \tag{19}$$

After some algebraic manipulation, Eqn 19 becomes:

$$\frac{V}{B} + 1 - \ln|R/a| = \sqrt{1+\frac{CR^2}{B^2}} - \ln\left|\frac{1}{2}\left(1+\sqrt{1+\frac{CR^2}{B^2}}\right)\right| \quad . \tag{20}$$

At this point, previous investigators[27-29] assumed that a first order expansion of the term $\sqrt{1+CR^2/B^2}$ was valid, and thus:

$$\frac{V}{B} + 1 - \ln(R/a) \simeq 1 + \frac{CR^2}{4B^2} , \tag{21}$$

or:

$$C = \frac{i}{2\pi\epsilon\langle k\rangle} = \frac{4V_c(V-V_c)}{R^2 \ln(R/a)} . \tag{22}$$

Using this result for C, one may determine the range of voltages over which the approximation

$$\sqrt{1 + \frac{CR^2}{B^2}} \simeq 1 + \frac{CR^2}{2B^2}$$

is valid. This expansion will be accurate (±10%) provided that $CR^2/B^2 \leq 1.3$. From Eqn 22,

$$\frac{CR^2}{B^2} = 4\ln(R/a)\,\frac{V-V_c}{V_c} , \tag{23}$$

and thus $CR^2/B^2 \leq 1.3$ requires that the applied voltage be less than $1.07\ V_c$ for the values of R and a encountered in this work (R = 1.9 cm, $a = 6.35 \times 10^{-3}$ cm). Thus, it is apparent that the previously noted approximation will have a very limited range of accuracy.

A more useful result may be obtained by considering the range of values for the parameter $\sqrt{1+CR^2/B^2}$. Letting $\lambda = \sqrt{1+CR^2/B^2}$, Eqn 20 may be written as:

$$\frac{V}{V_c} \ln|R/a| + 1 - \ln|R/a| = \lambda - \ln\left|\frac{1}{2}(1+\lambda)\right| . \qquad (24)$$

If we limit the values of V to $1.05V_c \leq V \leq 3V_c$, which encompass the typical values encountered in this work, the upper and lower bounds of λ (λ_u and λ_L, respectively) may be determined from:

$$\frac{1.05V_c}{V_c} \ln|R/a| + 1 - \ln|R/a| = \lambda_L - \ln\left|\frac{1}{2}(1+\lambda_L)\right|$$

and

$$\frac{3V_c}{V_c} \ln|R/a| + 1 - \ln|R/a| = \lambda_u - \ln\left|\frac{1}{2}(1+\lambda_u)\right| .$$

Solution of these equations yields

$$\lambda_L = 1.515$$

$$\lambda_u = 14.45$$

One may now perform a series expansion of the logarithmic term in order to obtain a rational function of λ. It is useful to express $\ln|(1+\lambda)/2|$ as

$$\ln|(1+\lambda)/2| = \ln\left|b + (\frac{\lambda+1}{2} - b)\right|$$

and expand about b to give:

$$\ln\left|b + (\frac{\lambda+1}{2} - b)\right| = \ln b + 2[\frac{\lambda'}{2b+\lambda'} + \frac{1}{3}(\frac{\lambda'}{2b+\lambda'})^3 \ldots .] \qquad (25)$$

which converges for

$$-a < \lambda' = (\frac{\lambda+1}{2} - b) < \infty, \text{ and } b > 0.$$

Truncating the expansion at two terms gives:

$$\ln(1/2(1+\lambda)) \simeq \ln b + \frac{\lambda+1-2b}{b+1/2(\lambda+1)} \quad . \tag{26}$$

Through iterative techniques, it was found that b=2 provided the best convergence for the series at λ_u and λ_L. Using b=2 will incur a 3.5% error at the lower bound of λ and an 8% error at the upper bound. These errors are felt to be tolerable in the forthcoming calculations, and thus this approximation will be used, allowing us to express Eqn 24 as:

$$(\frac{V}{V_c} - 1)\ln(R/a) + 1 = \lambda - \ln 2 - \frac{\lambda-3}{1/2\lambda+5/2} \quad .$$

Solving for λ gives:

$$\lambda = \frac{\Omega-3+\sqrt{\Omega^2+14\Omega-15}}{2} \tag{27}$$

where

$$\Omega = (\frac{V}{V_c} - 1)\ln(R/a) + 1 + \ln 2 \quad .$$

Recalling that $\lambda = \left(\frac{1+CR^2}{B^2}\right)^{1/2}$, (where $C = i/2\pi\epsilon\langle k\rangle$ and $B = V_c/\ln(R/a)$) and solving Eqn 27 for $i/2\pi\epsilon\langle k\rangle$ gives

$$\frac{i}{2\pi\epsilon\langle k\rangle} = \left(\frac{V_c}{R\ln(R/a)}\right)^2 \left(\left(\frac{\Omega-3+\sqrt{\Omega^2+14\Omega-15}}{2}\right)^2 - 1\right) \quad . \tag{28}$$

Since $\Omega \alpha (V/V_c - 1)$, this equation is of the form predicted by Tikhodejev[34] for the generalized current-voltage characteristics of a corona discharge:

$$\frac{I}{\varepsilon_o \langle k \rangle} \alpha V_c^2 f\left(\frac{V}{V_c} - 1\right) .$$

Letting $$F(V,V_c,R,a) = \left(\frac{V_c}{R\ln(R/a)}\right)^2 \left(\left(\frac{\Omega - 3 + \sqrt{\Omega^2 + 14\Omega - 15}}{2}\right)^2 - 1\right)$$

one may express the electric field in a coaxial cylinder corona discharge as:

$$X(r) = \left(F(V,V_c,R,a) + \left(\frac{V_c}{r\ln(R/a)}\right)^2\right)^{1/2} . \qquad (29)$$

Further, if one assumes that the total current is distributed equally over the length of the discharge tube (i.e. $i = I_T/L$), the mean ionic mobility may be determined from current-voltage data by:

$$I_T = 2\pi\varepsilon L \langle k \rangle F(V,V_c,R,a) . \qquad (30)$$

Since it is difficult to determine the mean ionic mobility from first principles, Eqn 30 will provide a useful method for determining $\langle k \rangle$ for a variety of gases.

Although Eqn 29 and Eqn 30 have been derived for specific conditions ($R = 1.9$ cm, $a = 6.35 \times 10^{-3}$ cm and $1.05V_c \leq V \leq 3V_c$), the

method used to derive these equations may easily be modified for applicability to discharge tubes of different dimensions, and for different voltage ranges.

Through the use of Eqn 29, an accurate evaluation of the electric field in a cylindrical corona discharge tube is possible. With this formulation for the electric field, we may now determine the acceleration an electron experiences between collisions with gas molecules. However, in order to describe the electron energy distribution, it is important to know the collision cross sections and the energy loss during collisions.

Electron Energy Distribution Function

The total cross section for the collision of electrons with molecules is the sum of the cross sections for individual processes[35]:

$$Q_T = Q_{elastic} + Q_{ionization} + Q_{excitation} + Q_{attachment} \cdots$$

where all terms but $Q_{elastic}$ may be summed together as $Q_{inelastic}$.

In order to accurately determine the electron energy distribution function (eedf) in the case where cross sections are energy dependent and inelastic collisions occur, solution of the Boltzmann-Maxwell transport equation is required[36]. In vectoral form, the equation may be written as[37]:

$$\frac{\partial F}{\partial t} + \bar{V} \cdot \nabla_r F + \frac{e\bar{X}}{m} \cdot \nabla_v F = \left(\frac{\partial F}{\partial t}\right)_c \qquad (31)$$

where F is the eedf, ∇_r and ∇_v are the gradient operators in coordinate and velocity space, respectively, and $\left(\frac{\partial F}{\partial t}\right)_c$ is the change in the distribution function at the instant of collision. The solution of Eqn 31 is inevitably quite complicated, and involves numerical techniques.

Two approximations to the solution of Eqn 31 are particularly useful[35], depending on the range of electric fields and the type of gas present. These are the Druyvesten[38] and the Maxwellian[39] distributions. The Druyvesten distribution may be derived from the Boltzman transport equation by assuming that the collision cross section is a constant. If the collision frequency is held constant, the solution to the transport equation will have the form of a Maxwellian distribution.

In highly ionized gases, the electrons tend to "thermalize" independent of the neutral gas since the effects of electron-electron collisions dominate those of electron neutral collisions[35]. In slightly ionized gases, either of these distributions may be applicable, depending on the collison properties of the gas. In order to determine which of these distributions would be most applicable in methyl iodide/ nitrogen gas streams, it was useful to consider some of the previous experimental results in this field.

The electron energy distribution function in the methyl iodide/nitrogen mixtures used in this work is assumed to be the same as

that in pure N_2, since the methyl iodide concentrations are very low[40]. The eedf in nitrogen has been found to have the same shape as that in argon for high values of the electric field[41] ($\chi \geq 1000$ V/cm at atmospheric pressure). Since the Druyvesten distribution is known to provide a good approximation to the electron energy distribution function in argon[42], this distribution has been used for the eedf in nitrogen in this work. The average energy term in the Druyvesten distribution was evaluated from experimental data[43a-d], and fitted (by least squares) as a function of the electric field. From this, the electron energy distribution function was determined to be:

$$f(E,\chi)dE = E^{1/2} \exp - 0.548 \left(\frac{E}{\langle E \rangle}\right)^2 dE \qquad (32)$$

where the average electron energy may be evaluated for any given electric field from (see Figure 1):

$$\langle E \rangle = C_1\sqrt{\chi} + C_2$$

where:

$C_1 = 0.0270\pm0.001 \frac{ev}{(V/cm)^{1/2}}$, $C_2 = 0.033\pm0.009$ ev, $400 \leq \chi \leq 1.37\times10^3$ V/cm

$C_1 = 0.012\pm0.001 \frac{ev}{(V/cm)^{1/2}}$, $C_2 = 0.494\pm0.040$ ev, $1.37\times10^3 \leq \chi \leq 2.26\times10^4$ V/cm

$C_1 = 0.031\pm0.002 \frac{ev}{(V/cm)^{1/2}}$, $C_2 = -2.36\pm0.39$ ev, $\chi > 2.26\times10^4$ V/cm .

Making the two assumptions that the eedf in argon and nitrogen are similar in form, and that it is unaffected by low concentrations of

FIGURE 1 relates the mean energy of electrons in nitrogen (at 300 K and 760 torr) to the square root of the electric field. Experimental data were obtained from references 43(a)-43(d). The solid lines indicated are least squares fits to the experimental data, and are given by the fitting parameters indicated in the text.

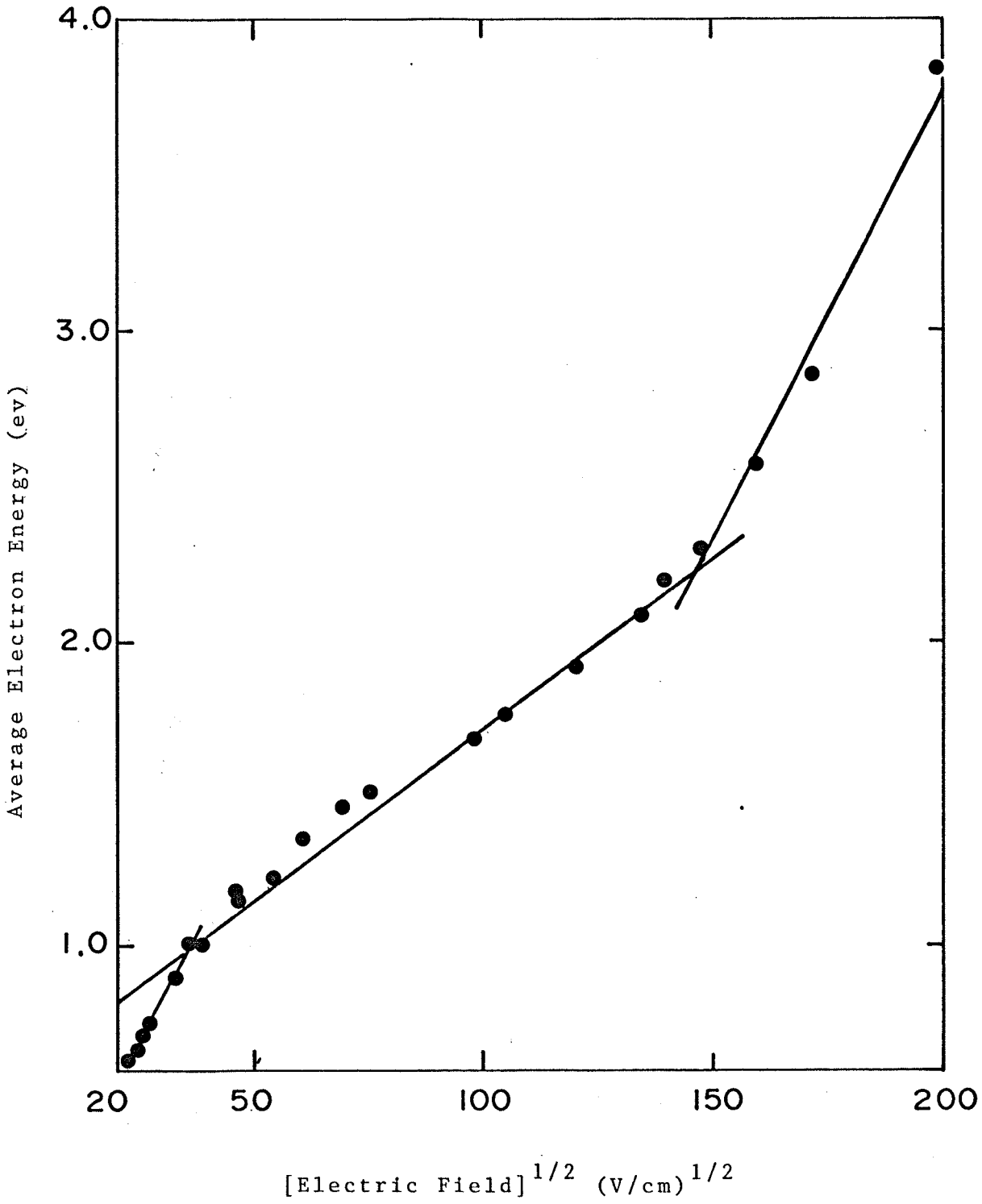
4.0
3.0
2.0
1.0
Average Electron Energy (ev)
20
50
100
150
200
[Electric Field]$^{1/2}$ (V/cm)$^{1/2}$

CH_3I, the Druyvesten distribution normalized to experimental measurements of $\langle E \rangle$ in N_2 will provide an adequate approximation to the eedf, especially in the low energy tail of the distribution.

Decomposition of Methyl Iodide

With this knowledge of the electron energy distribution and the electric field, we may now model the decomposition of methyl iodide in nitrogen in a corona discharge.

The decomposition of methyl iodide in the corona discharge occurs through two different processes, each predominant in different regions of the discharge. In the drift region of the discharge (which encompasses the majority of the discharge tube volume), the mean electron energies are low ($\sim$ 1 ev), and dissociative electron capture:

$$CH_3I + e \rightarrow CH_3 + I^- \qquad \Delta H = -0.62 \text{ ev}$$

will be the major electron-molecule interaction. Reactions which require energetic electrons such as:

$$CH_3I + e \rightarrow CH_3 + I + e \qquad \Delta H = 2.58 \text{ ev}^{(44)}$$
$$\rightarrow CH_3I^+ + 2e \qquad \Delta H = 9.6 \text{ ev}^{(45)}$$

or reactions initiated by energy storage in nitrogen metastable states:

$$N_2 + e \rightarrow N_2^* + e \qquad \Delta H = 6.7 \text{ ev}^{(46)}$$
$$N_2^* + CH_3I \rightarrow N_2 + \text{products}$$

will occur principally in regions of high electric field (i.e. quite close to the filament).

(i) Dissociative Electron Capture

The dissociative capture of electrons by methyl iodide may be modelled quite rigorously, provided the electron energy distribution is known and the capture cross section is known as a function of electron energy ($\sigma(E)$). In order to do so, we may first consider the reaction of mono-energetic electrons of energy E with an electron attaching gas of concentration C, which may be treated as a bimolecular reaction with rate:

$$R(E) = \sigma(E)\, v_e(E)\, C_e\, C \qquad (33)$$

where $v_e(E)$ is the electron velocity ($(2E/m_e)^{1/2}$), and C_e is the electron concentration.

To account for the distribution of electron energies, the velocity-weighted, energy-averaged cross section[40] has been employed, to give:

$$\langle R(r)\rangle = \sigma_V(r)\langle v_e C_e\rangle C \qquad (34)$$

where $\sigma_V(r)$ is defined as:

$$\sigma_V(r) = \frac{\int_0^\infty \sigma(E) E^{1/2} f(E,\chi)\, dE}{\int_0^\infty E^{1/2} f(E,\chi)\, dE} \,. \qquad (35)$$

The averaged rate and cross section are expressed as functions of r since the energy distribution ($f(E,\chi)$) depends on the electric field, which is a function of the radial coordinate. The subscript V on the cross section indicates a constant applied voltage.

The electron capture cross section for methyl iodide may be approximated by a gaussian distribution with centroid at 0.15 ev and a full width at half maximum of 0.30 ev[47]. Thus:

$$\sigma(E) \simeq \sigma_{max} \exp\left(-\left(\frac{E-0.15}{0.18}\right)^2\right) \tag{36}$$

and Eqn 35 may be expressed as:

$$\sigma_V(r) \simeq \sigma_{max} \frac{\int_0^\infty E \exp\left(-\left(\frac{E-0.15}{0.18}\right)^2\right) \exp - 0.548\left(\frac{E}{\langle E\rangle}\right)^2 \, dE}{\int_0^\infty E \exp - 0.548\left(\frac{E}{\langle E\rangle}\right)^2 \, dE} . \tag{37}$$

In Eqn 37, σ_{max} is the electron capture cross-section for E = 0.15 ev, and the average value of E ($\langle E\rangle$) is as defined previously. Making the substitutions:

$$E = 0.18\ Y, \quad \nu = \frac{-0.15}{0.18} = -0.833, \text{ and } \mu = \sqrt{1 + \left(\frac{0.1332}{\langle E\rangle}\right)^2},$$

Eqn 37 may be expressed as:

$$\sigma_V(r) = \frac{1.77\times10^{-2}\ \sigma_{max}}{\langle E\rangle^2}\int_0^\infty Y\ \exp(-\mu Y^2-2\nu Y)dY \quad . \tag{38}$$

Integration of Eqn 38 gives[48]

$$\sigma_V(r) = \frac{1.77\times10^{-2}\ \sigma_{max}}{\langle E\rangle^2}\left(\frac{1}{2\mu} - \frac{\nu}{2\mu}\sqrt{\frac{\pi}{\mu}}\ e^{\nu^2/\mu}[1-\Phi(\nu/\sqrt{\mu})]\right) , \tag{39}$$

where Φ is the gamma function.

For the values of χ encountered in our experiments, the average value of the electron energy is greater than 0.5 ev, and thus:

$$e^{\nu^2/\mu}[1-\Phi(\nu/\sqrt{\mu})] \simeq 3.45 \quad .$$

With some algebraic manipulation, Eqn 39 becomes:

$$\sigma_V(r) = 8.85\times10^{-3}\ \sigma_{max}\left(\frac{1}{\langle E\rangle^2+(0.1332)^2} + \frac{5.09\langle E\rangle}{(\langle E\rangle^2+(0.1332)^2)^{3/2}}\right). \tag{40}$$

Returning to Eqn 33, and expressing the product $\langle V_e C_e\rangle$ as the current density of electrons J_e, we may write:

$$\langle R(r)\rangle = \sigma_V(r)\ Je\ C \quad . \tag{41}$$

Using cylindrical polar coordinates, the current density of electrons at position (r,z) may be expressed as:

$$J_e = \frac{i_e(r,z)}{2\pi r} \tag{42}$$

where $i_e(r,z)$ is the electron current per unit length of discharge tube at position (r,z).

The form of $i_e(r,z)$ may be deduced by first considering a current of mono-energetic electrons (I_e) attaching to gas molecules of concentration C as they traverse a distance dr:

$$\frac{di_e(r,z)}{dr} = -\sigma(E)\, i_e(r,z)\, C \quad . \tag{43}$$

Multiplying both sides of this equation by $E^{1/2}\, f(E,X)dE$ and integrating over the energy gives:

$$\frac{di_e(r,z)}{dr} = -\sigma_V(r) i_e(r,z)\, C \quad . \tag{44}$$

Integration of Eqn 44 yields:

$$i_e(r,z) = \frac{I_T}{L} \exp\left(-C \int_a^r \sigma_V(r)dr\right) \tag{45}$$

where I_T is the total current, L is the length of the discharge tube, and I_T/L is the electron current per unit length at the filament. In Eqn 45, it has been assumed that the concentration of the attaching species is independent of the radial coordinate, and that the current is distributed uniformly over the length of the discharge tube. These assumptions are justified by experimental observations.

Substitution of Eqns 42 and 45 into Eqn 41 gives:

$$\langle R(r)\rangle = \sigma_V(r) \frac{I_T}{2\pi rL} C \exp\{-C \int_a^r \sigma_V(r)dr\} \quad . \tag{46}$$

The rate of change of concentration of electron attaching molecules due to dissociative capture in a volume element $d\tau$ is:

$$\frac{dC}{dt} d\tau = -\sigma_V(r) \frac{I_T}{2\pi rL} C \exp(-C \int_a^r \sigma_V(r)dr)d\tau \quad . \tag{47}$$

Eqn 47 is equivalent to

$$\frac{dC}{dz} \frac{F}{(R^2-a^2)} 2rdr = -\sigma_V(r) \frac{I_T}{L} C \exp(-C \int_a^r \sigma_V(r)dr)dr \tag{48}$$

since $\frac{dC}{dt} = \frac{dC}{dz}\frac{dz}{dt} = \frac{dC}{dz}\frac{F}{\pi(R^2-a^2)}$, and $d\tau = 2\pi rdrdz$.

Integration over r and making appropriate cancellations yields:

$$\frac{dC}{dz} = \frac{I_T}{LF}\left(\exp\left(-C\int_a^R \sigma_V(r)dr\right) - 1\right). \qquad (49)$$

Thus, the rate of change of concentration (by dissociative electron capture) with respect to the distance down the discharge tube may be determined provided one is able to evaluate the integral $\int_a^R \sigma_V(r)dr$. In this work, this integral was evaluated numerically through the use of an adaptive iterative code based on Simpson's rule[49].

(ii) High Energy Processes

The high energy processes may all be described in terms of bimolecular rates, i.e. $R_i = k_i I_T C$, where k_i is a parameter related to the cross-section for the i^{th} reaction channel. For bimolecular reactions between electrons and the molecular reactant, the rate may be written as:

$$R(r,z) = \sum_i \frac{\int_o^\infty \sigma_i(E)E^{1/2}f(E,\chi)dE}{\int_o^\infty E^{1/2}f(E,\chi)dE} \langle VC_e \rangle \quad C \qquad (50)$$

where $\sigma_i(E)$ is the cross section of the i^{th} reaction channel as a function of electron energy, and C is the concentration of the molecular reactant.

Since these reactions require a high electron energy ($E \geq D(CH_3\text{-}I) = 2.58$ ev), they will predominantly occur near the filament. In this region, the electric field is relatively independent of the applied voltage[30], and depends solely on V_c (see Figure 2). This implies that the convolution of $\sigma_i(E)$ with $f(E,\chi)$ will be independent of the voltage. Furthermore, electron capture will be a minor process in the ionization sheath (due to the high electron energies in this zone), and thus the negative current will consist entirely of electrons. Using $J = \langle VC_e \rangle = I_T/2\pi rL$, Eqn 50 becomes:

$$R(r,z) = \sum_i \frac{\int_o^\infty \sigma_i(E) E^{1/2} f(E,\chi) dE}{\int_o^\infty E^{1/2} f(E,\chi) dE} \frac{I_T}{2\pi rL} C \quad . \tag{51}$$

Since the rate of decomposition of molecular reactant in a volume element $d\tau$ is equal to $-R(r,z)d\tau$, we may express Eqn 49 as:

$$\frac{dC}{dZ} \frac{F}{\pi R^2} d\tau = -\sum_i \frac{\int_o^\infty \sigma_i(E) E^{1/2} f(E,\chi) dE}{\int_o^\infty E^{1/2} f(E,\chi) dE} \frac{I_T}{2\pi rL} C \, d\tau \quad . \tag{52}$$

Finally, if we consider those high energy processes only occurring within a distance r_1 of the filament (i.e. the region in which the electric field is large enough that the energy integrated cross section of these reactions is significant), Eqn 52 may be integrated to give:

FIGURE 2 relates the electric field in the ionization sheath of a co-axial cylinder discharge tube to the distance from the high voltage electrode. The electric fields were calculated from Eqn 29, assuming that V_c = 5.0 kV, R = 1.9 cm and a = 6.35×10^{-3} cm. A comparison is made between the field at onset of the discharge (V = 5 kV), and the field when the applied voltage is 10 kV.

——— V = 5 kV

----- V = 10 kV

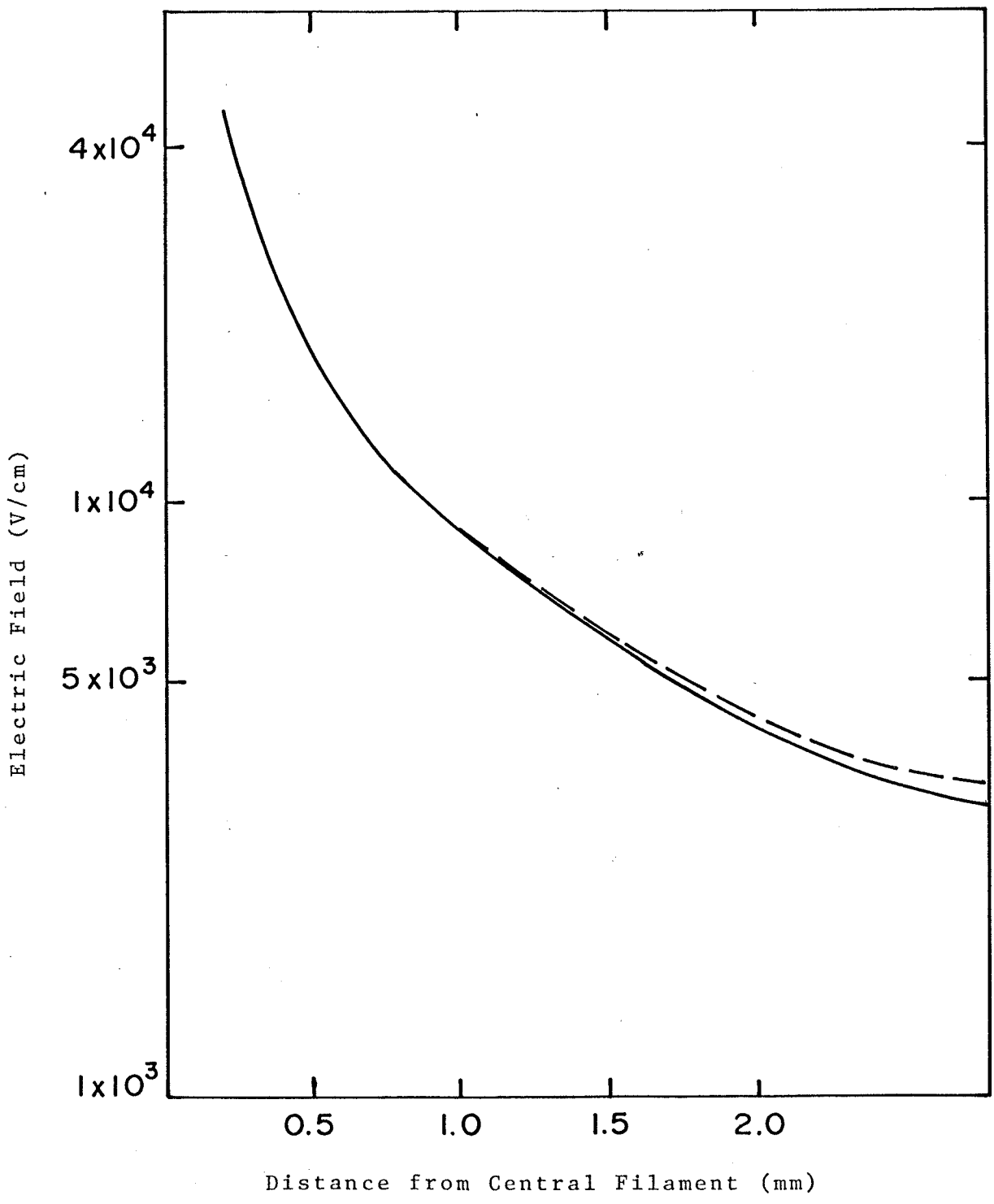
4x10^4
1x10^4
5x10^3
1x10^3
Electric Field (V/cm)
0.5
1.0
1.5
2.0
Distance from Central Filament (mm)

$$\frac{dC}{dz} = \frac{-R^2}{(r_1^2-a^2)} \frac{I_T}{FL} C \int_a^{r_1} \sum_i \frac{\int_o^\infty \sigma_i(E)E^{1/2} f(E,\chi)dE}{\int_o^\infty E^{1/2} f(E,\chi)dE} dr = -K \frac{I_T}{FL} C$$

where

$$K = \frac{R^2}{r_1^2-a^2} \int_a^{r_1} \sum_i \frac{\int_o^\infty \sigma_i(E)E^{1/2} f(E,\chi)dE}{\int_o^\infty E^{1/2} f(E,\chi)dE} dr \quad . \tag{53}$$

Combining Eqn 53 with Eqn 49 gives the total change in concentration of molecular reactant in the axial direction:

$$\frac{dC}{dz} = -\frac{I_T}{LF}\left(KC + 1 - \exp -C \int_a^R \sigma_V(r)dr\right) . \tag{54}$$

Recalling that $dz/dt = F/\pi R^2$, one may determine the time rate of change of methyl iodide concentration (due to electron-molecule interactions) by multiplying Eqn 54 by dz/dt, giving

$$\frac{dC}{dt} = -\frac{I_T}{\pi R^2 L}\left(K\,C + 1 - \exp -C \int_a^R \sigma_V(r)dr\right) . \tag{55}$$

Although Eqn 55 may be used to describe the initial rate of decomposition of methyl iodide, one must also consider the subsequent reactions of species formed during the decomposition processes in order to adequately describe the system.

One might expect that there would be similarities between the system under investigation and the photolytic decomposition of methyl iodide[50-53], with electron-molecule interactions replacing photon-molecule interactions as the initiating process. Thus, one may propose the following general mechanism to explain the overall rate of decomposition of methyl iodide in a corona discharge:

$$CH_3I + e \rightarrow CH_3 + I^- \quad (R1)$$

$$CH_3I + e \rightarrow CH_3 + I + e \quad (R2)$$

$$CH_3 + I \overset{M}{\rightarrow} CH_3I \quad (R3)$$

$$CH_3 + CH_3 \rightarrow C_2H_6 \quad (R4)$$

$$I + I \overset{M}{\rightarrow} I_2 \quad (R5)$$

$$CH_3 + I_2 \rightarrow CH_3I + I \quad (R6)$$

$$CH_3 + CH_3I \rightarrow CH_4 + CH_2I \quad (R7)$$

$$CH_2I + I \overset{M}{\rightarrow} CH_2I_2 \quad (R8)$$

$$CH_2I + I_2 \rightarrow CH_2I_2 + I \quad (R9)$$

$$CH_2I + CH_3 \rightarrow C_2H_5I \quad (R10)$$

$$CH_2I + CH_2I \rightarrow C_2H_4I_2 \quad (R11)$$

$$CH_3 + CH_3I \rightarrow C_2H_6 + I \quad (R12)$$

$$CH_2I + CH_3I \rightarrow CH_2I_2 + CH_3 \quad (R13)$$

$$CH_3 + CH_2I \rightarrow C_2H_4 + HI \quad (R14)$$

$$I + CH_3I \rightarrow CH_3 + I_2 \quad (R15)$$

$$I + CH_3I \rightarrow HI + CH_2I \quad (R16)$$

$$I^- \rightarrow I_{(ads)} \quad (R17)$$

$$I \rightarrow I_{(ads)} \quad (R18)$$

$$I_2 \rightarrow I_{2(ads)} \quad (R19)$$

where M is a third body, and the subscript (ads) indicates that the species is physically (or chemically) adsorbed on the wall of the discharge tube.

The feasibility of this mechanism was investigated throughout the course of the experimental studies in an effort to determine the rate-controlling steps and principal reactions involved in the corona-induced decomposition of methyl iodide.

EXPERIMENTAL

The experimental apparatus used in this study may be divided into three regions of interest:

1) the gas handling system,
2) the discharge tube, and
3) the gas analysis region.

The gas handling system (see Figure 3) allowed for the production of nitrogen/methyl iodide mixtures of known flow rate and methyl iodide concentration. The methyl iodide (Alfa Products, 99% purity) used was further purified by vacuum distillation, while the nitrogen (Canadian Liquid Air, 99.999% purity) was purified by passing it through an oxygen trap to remove any residual O_2 (final $[O_2] < 20$ μL/L). Flow rates were measured using calibrated Matheson rotameters and/or a Matheson mass flowmeter.

FIGURE 3 Schematic Diagram of the Experimental Apparatus

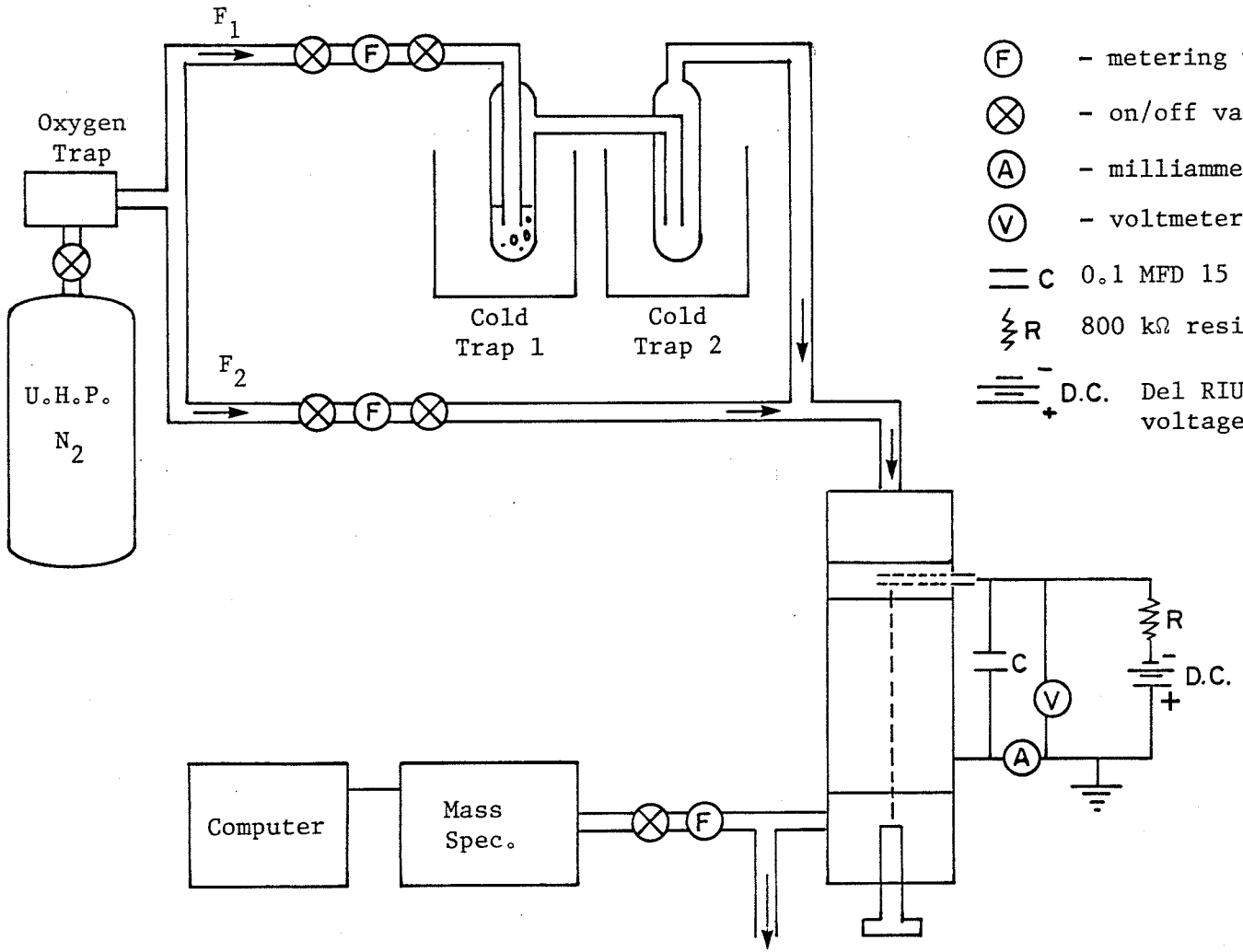
F1
F
Oxygen
Trap
Cold
Trap 1
Cold
Trap 2
F2
F
U.H.P.
N2
R
C
D.C.
V
A
Computer
Mass
Spec.
F
F - metering valve
- on/off valve
A - milliammeter
V - voltmeter
C 0.1 MFD 15 kV capacitor
R 800 kΩ resistor
D.C. Del RIU-875 high voltage power supply

The methyl iodide/nitrogen mixture was formed by saturating a nitrogen gas stream (F_1) with methyl iodide (at temperature T_1) and condensing some of the methyl iodide in a trap at temperature T_2 ($T_1 > T_2$). Temperature control during the saturation and condensation steps was provided in two different ways: firstly, by using slush baths, and secondly, by using commercial constant temperature baths (Neslab Cryocool Service). The flow F_1 was subsequently added to the bulk nitrogen flow F_2. The concentration of methyl iodide in the total gas flow was calculated from the vapour pressure of methyl iodide[54] and the flows F_1 and F_2.

The methyl iodide/nitrogen mixture was flowed through the discharge region of the apparatus (see Figure 3). Two cylindrical discharge tubes (see Figures 4 and 5) were used, one fabricated from copper, and the other from stainless steel. The copper tube was prepared by operating the corona discharge in a flow of CH_3I/N_2 for a few days. Thereafter, reproducible results were obtained that agreed with the stainless steel tube results. The high voltage electrode was a 1.3×10^{-2} cm diameter tungsten wire held under spring tension along the axis of the cylinder. The output from a Del (RIU 875) High Voltage D.C. power supply was smoothed using an 800 kΩ resistor and a 0.1 μF capacitor (see Figure 3). The voltage and current were the measured discharge parameters.

Gas analysis was provided by an Extranuclear quadrupole mass spectrometer, which sampled the gas as it left the discharge region. Data acquisition and analysis was performed on an LSI 11/23 computer interfaced to the mass spectrometer.

FIGURE 4 Schematic diagram of a coaxial cylinder discharge tube, with dimensions:

$a - 6.35 \times 10^{-3}$ cm

R - 1.9 cm

L - 46 cm

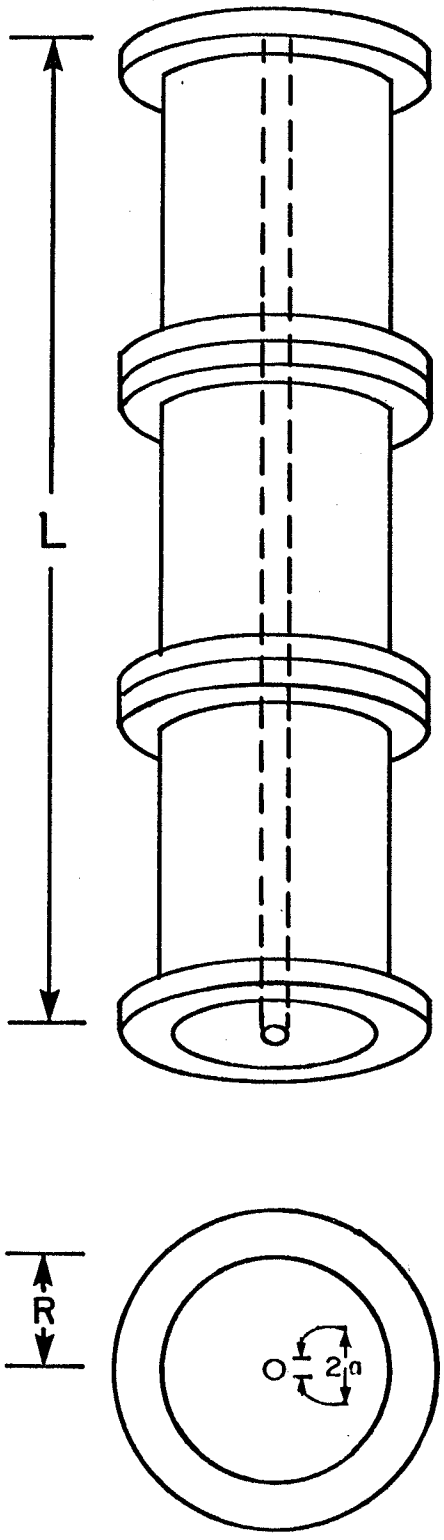
L
R
2a

The majority of experiments performed involved determining the amount of methyl iodide removed as a function of the operating parameters:

(i) initial methyl iodide concentration, C_o,

(ii) bulk gas flow rate, F,

(iii) discharge current, I, and

(iv) discharge voltage, V.

A set of experiments was performed to determine the nature and yield of discharge products. Quantitative yields were obtained by calibrating the mass spectrometer with commercially available samples of the expected product species.

In another set of experiments, short ($\sim$ 6.0 cm) segments of the discharge tube were electrically isolated from each other (see Figure 5). The current on each of these segments was measured, allowing for the determination of the current in various zones of the discharge tube.

The dependence of methyl iodide concentration on distance from the central axis of the tube was investigated by sampling the gas stream at different distances from the central filament. A section of the discharge tube was constructed with a radial sampling port, as shown in Figure 6. The sampling probe used was constructed from partially oxidized Zr tubing to prevent arcing.

FIGURE 5 A schematic diagram indicating the modifications made to a coaxial cylinder discharge tube to determine the current distribution over the length of the discharge tube. The symbol (A) indicates a milliammeter.

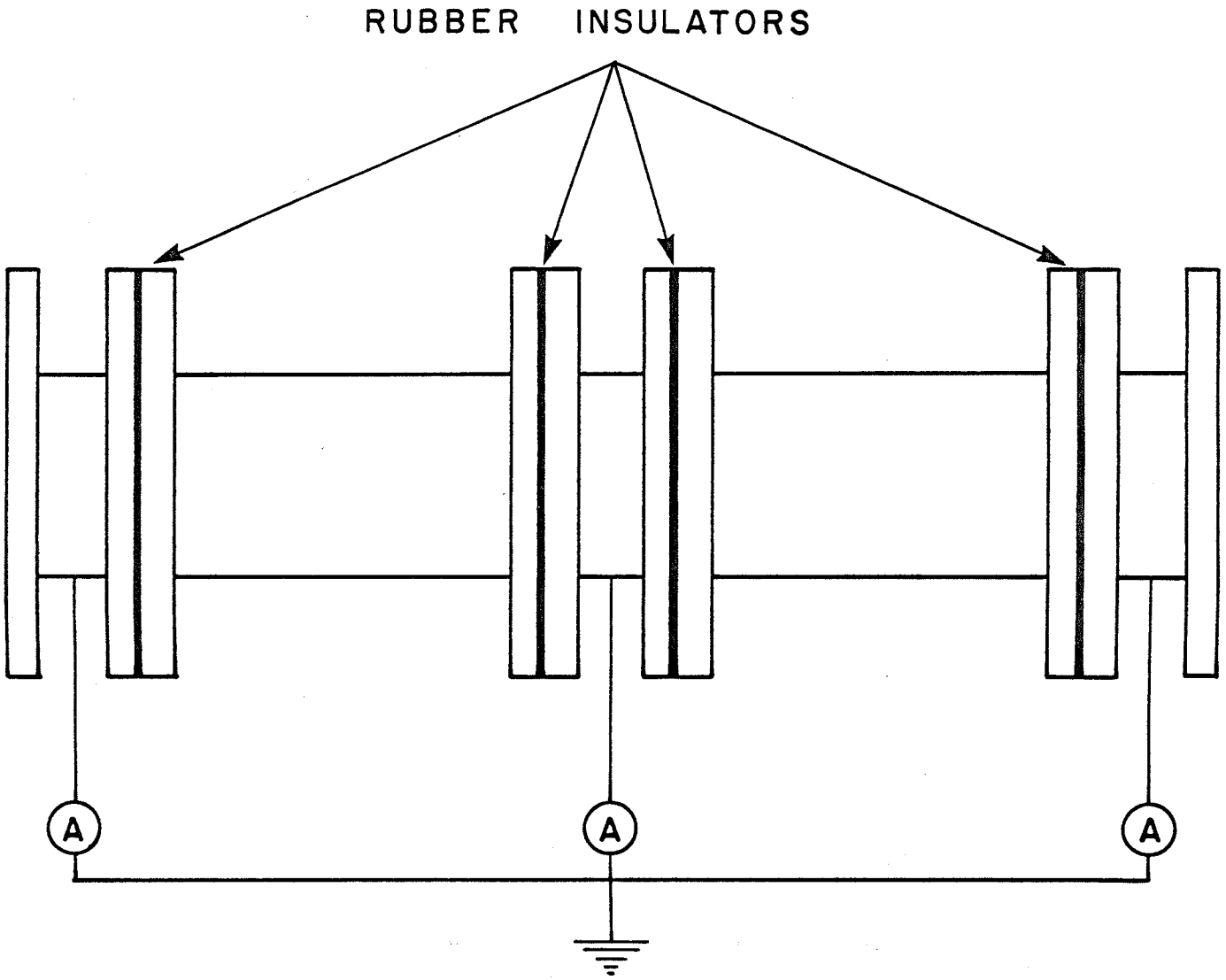
RUBBER INSULATORS
A
A
A

FIGURE 6 Section of discharge tube showing radial sampling apparatus.

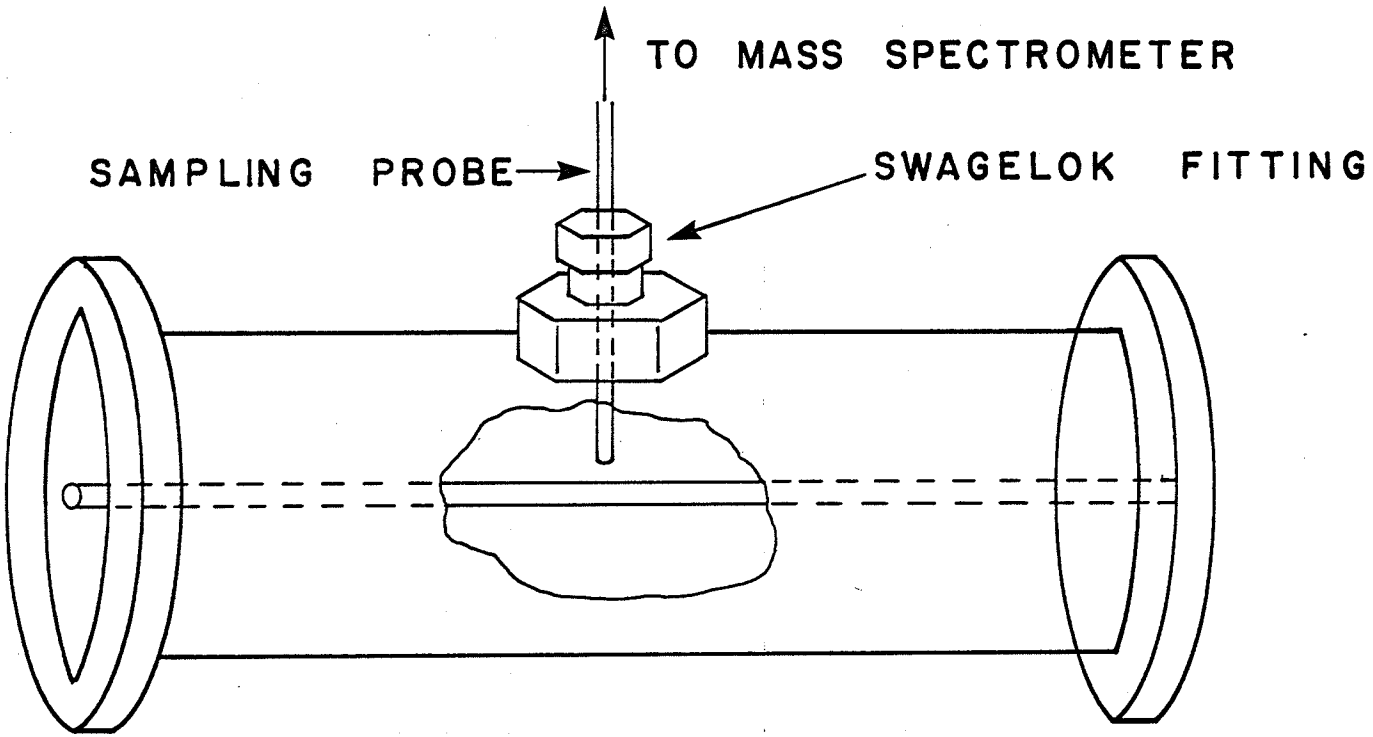
TO MASS SPECTROMETER
SAMPLING PROBE
SWAGELOK FITTING

RESULTS AND DISCUSSION

Prior to ascertaining the validity of the mechanism described in reactions R1-R19, numerous experiments were performed to investigate the assumptions employed in developing Eqn 54.

In order to evaluate the energy integrated, radially averaged, velocity-weighted electron capture cross section, an accurate description of the electric field is required. Previously in this work, an equation was derived which predicts the electric field in a coaxial cylinder corona discharge (Eqns 28 and 29). These equations may also be used to predict the current-voltage characteristics of the discharge (Eqn 30). Thus, a detailed current-voltage study was performed, and compared to the results of the derivation in order to ensure that Eqns 28 and 29 would suitably describe the electric field.

The current-voltage data were fitted to Eqn 30 by means of a non-linear curve fitting program[55], with the onset voltage, V_c, and mean ionic mobility, $\langle k \rangle$, as the fitting parameters. In all cases, it was found that Eqn 30 fit the current-voltage data quite accurately. Typical fits are given in Figures 7 to 9.

The onset voltage of the discharge was found to be independent of the initial concentration of methyl iodide, and was found to be 5.11 ± 0.12 kV, where the error quoted is the error in the mean value.

FIGURE 7 Current voltage data for the experimental conditions:

Initial methyl iodide concentration - 10 μL/L

Bulk gas flow rate - 2.0 L/min.

Dots are experimental values, and the solid line is the least squares fit to Eqn 30.

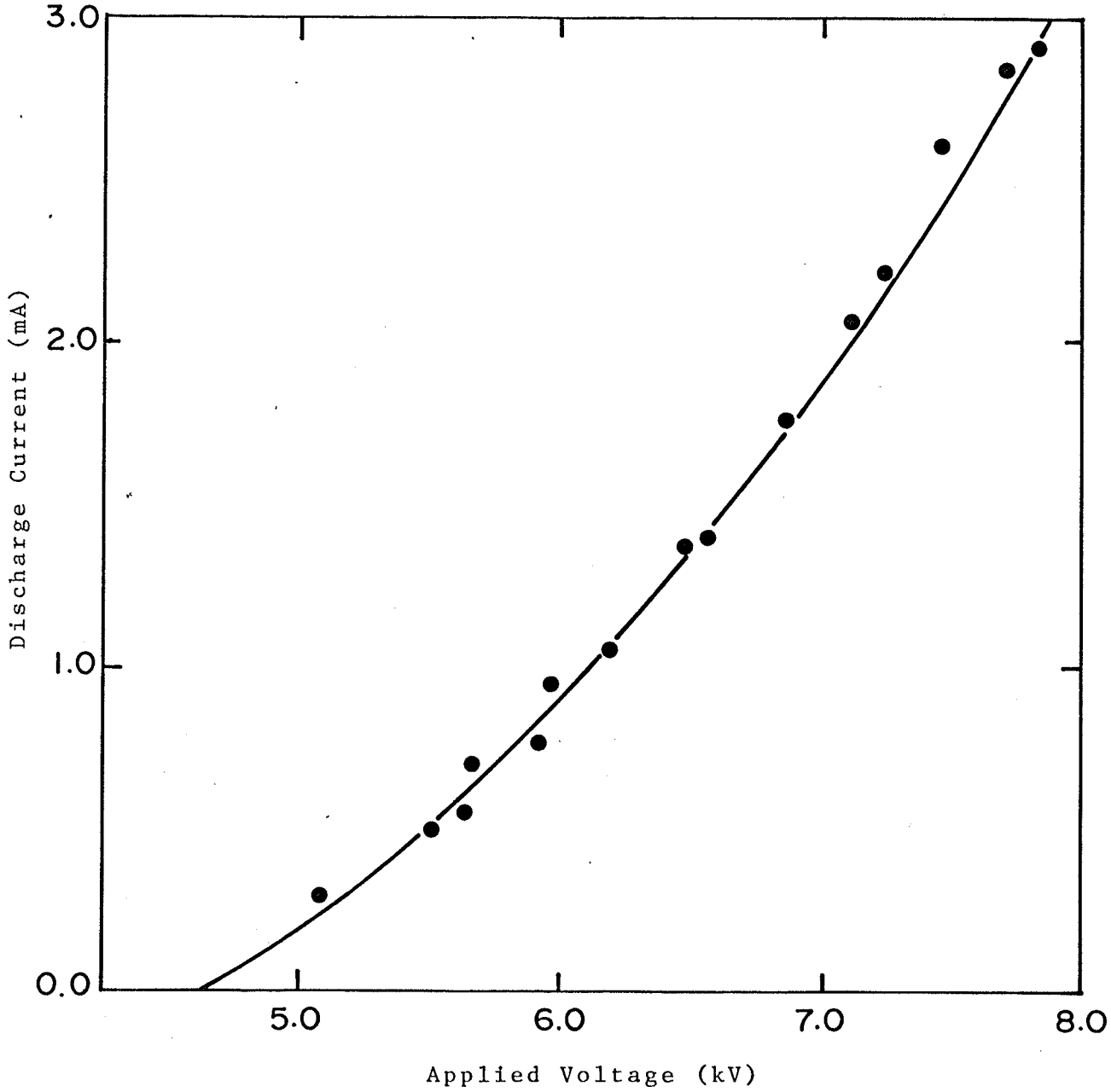
3.0
2.0
1.0
0.0
Discharge Current (mA)
5.0
6.0
7.0
8.0
Applied Voltage (kV)

FIGURE 8 Current voltage data for the experimental conditions:

Initial methyl iodide concentration - 53 µL/L

Bulk gas flow rate - 2.0 L/min

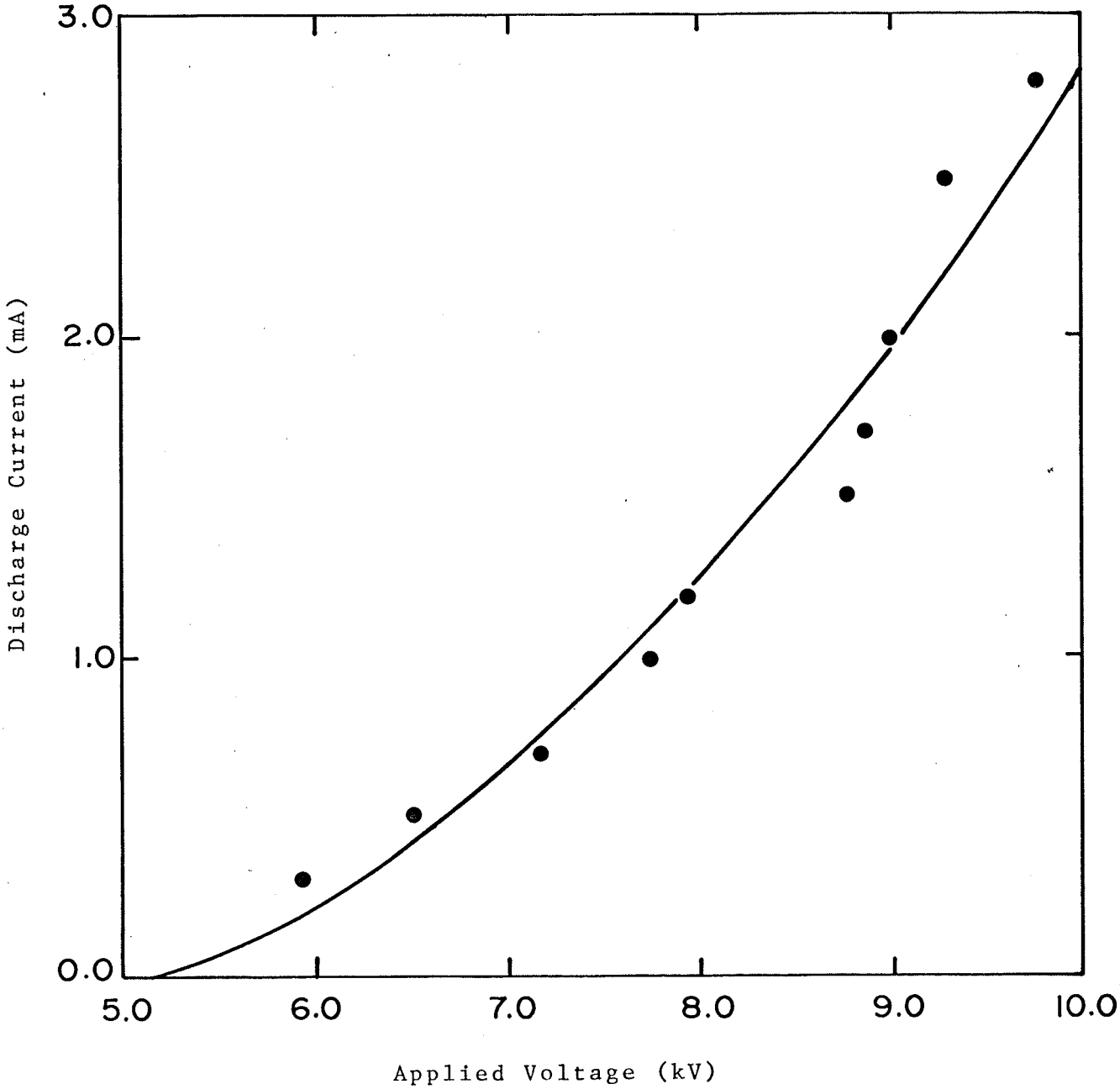
3.0
2.0
1.0
0.0
Discharge Current (mA)
5.0
6.0
7.0
8.0
9.0
10.0
Applied Voltage (kV)

FIGURE 9 Current voltage data for the experimental conditions:

Initial methyl iodide concentration - 200 µL/L

Bulk gas flow rate - 1.0 L/min

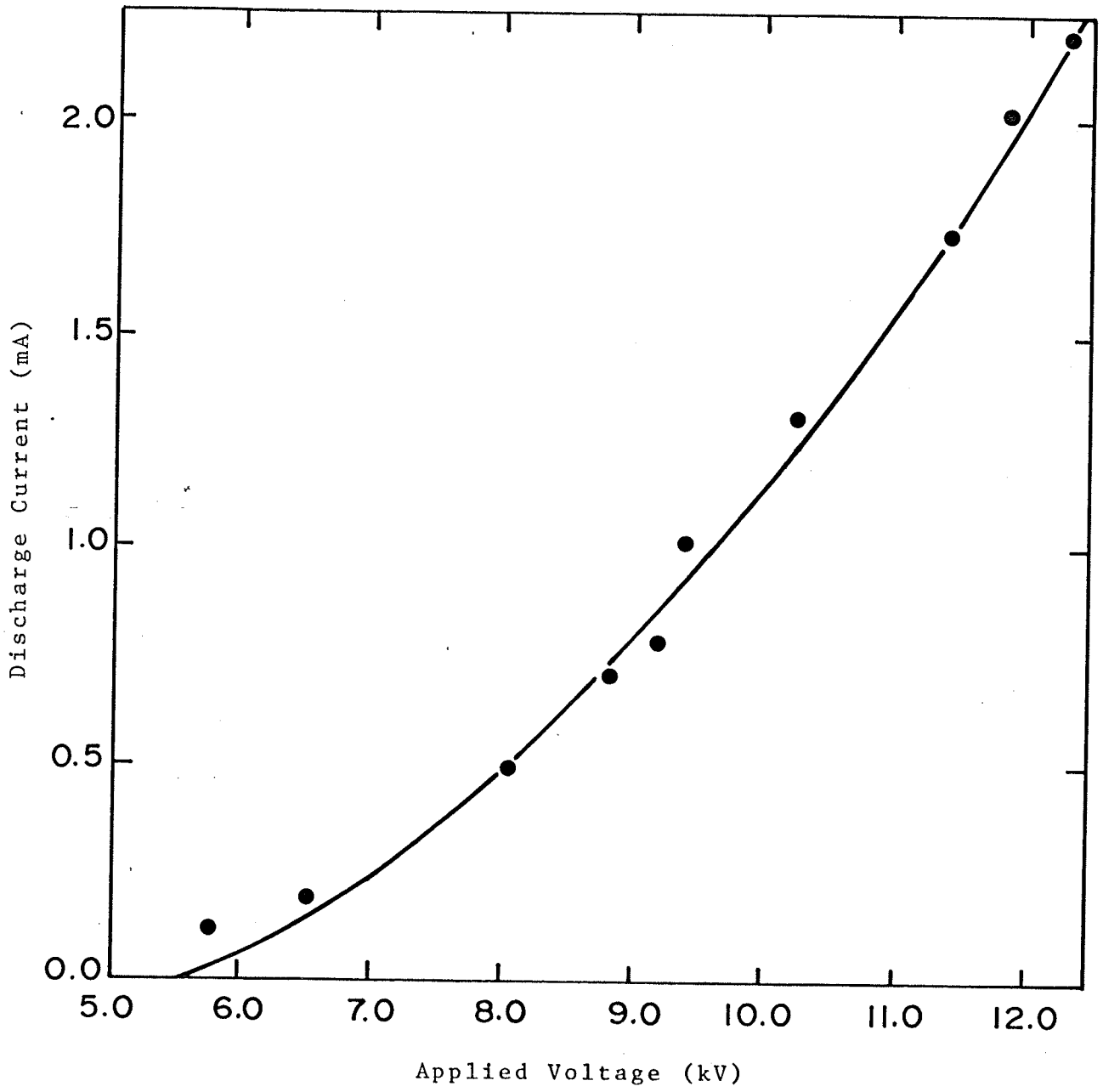
Discharge Current (mA)
2.0
1.5
1.0
0.5
0.0
5.0
6.0
7.0
8.0
9.0
10.0
11.0
12.0
Applied Voltage (kV)

The mean ionic mobility was found to be strongly dependent on the initial concentration of methyl iodide, and varied approximately as $1/C_o$ (see Figure 10). At the highest concentrations studied, the mean ionic mobility was 2.5 ± 0.1 $cm^2V^{-1}s^{-1}$, which is slightly greater than the mobility of I^- in N_2 at 760 torr. The y intercept of Figure 11 corresponds to the predicted mean mobility of ions in a discharge through pure methyl iodide, and shows excellent agreement with the mobility of I^- ($k \approx 2.3$ $cm^2V^{-1}s^{-1}$). This was the expected result, since I^- will be the predominant ion at high methyl iodide concentrations.

Since the model derived previously is capable of accurately predicting the current-voltage characteristics of the discharge, it will also provide reasonable values for the electric field at all points within the discharge tube.

The strong dependence of the mean ionic mobility on the methyl iodide concentration is due to the increased probability of electron capture processes when the methyl iodide concentration is large. This would suggest that more current could be carried through the region near the end of the discharge tube, rather than where the methyl iodide originally enters the system, since the concentration of methyl iodide is reduced as the gas flows down the tube. The model developed to describe the methyl iodide decomposition makes the assumption that the current is distributed equally along the length of the tube. In light of the previous argument, the validity of this assumption had to be verified experimentally.

FIGURE 10 The mean ionic mobility is plotted against the reciprocal of the initial methyl iodide concentration. The solid curve indicates a linear approximation to these data.

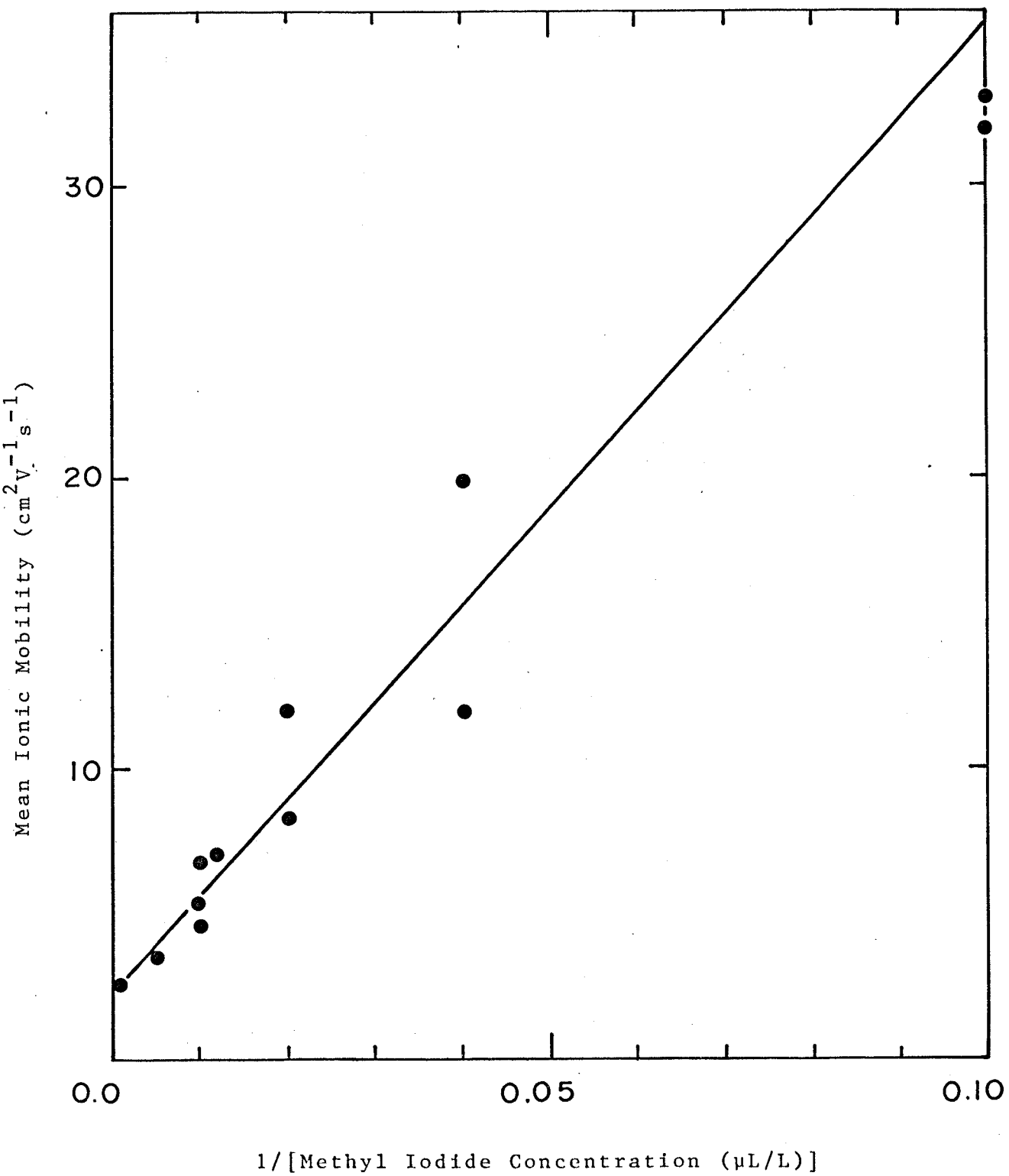
30
20
10
0.0
0.05
0.10
Mean Ionic Mobility ($cm^2 V^{-1} s^{-1}$)
1/[Methyl Iodide Concentration (μL/L)]

The worst case for this assumption will occur during experimental conditions of low flow rate and low initial concentrations, as these conditions provide for large percent changes in the methyl iodide concentration along the discharge tube. Figure 11 presents typical data obtained for the current per unit length near the entrance to the discharge tube ($0 \leq z \leq 6.0$ cm) and near the exit ($40 \leq z \leq 46$ cm). Also shown is the approximation used in developing the decomposition model, i.e. that the current per unit length is given by the total current divided by the length of the discharge tube. As can be seen in Figure 10, this approximation is reasonably accurate, and in extreme cases deviates from the experimental data by less than 10%.

One further assumption made in deriving Eqn 54 involves using a plug flow model to describe the change in methyl iodide concentration with respect to the radial coordinate. Thus, the model assumes that the CH_3I concentration will be constant radially at any point along the discharge tube.

The dependence of the methyl iodide concentration on the radial distance from the filament was investigated by sampling at various distances from the central axis of the discharge tube at a fixed distance along the tube. The volume of gas sampled per second was much less than the bulk flow ($\sim 2 \times 10^{-2}$ ml/s sampled from a 15.8 ml/s flow), and the ceramic sampling tube was of negligible size in comparison to the tube cross section. Thus, it was assumed that the sampling process did not affect the macroscopic properties of the discharge. The results of these experiments indicated that the methyl

FIGURE 11 Experimental data relating the current per unit length of discharge tube at two distances along the tube to the applied voltage.

○ 40.0 cm $\leq$ z $\leq$ 46.0 cm

● 0 cm $\leq$ z $\leq$ 6.0 cm

—— approximation used in this work

Experimental conditions:

Initial methyl iodide concentration - 30 μL/L

Bulk gas flow rate - 0.5 L/min

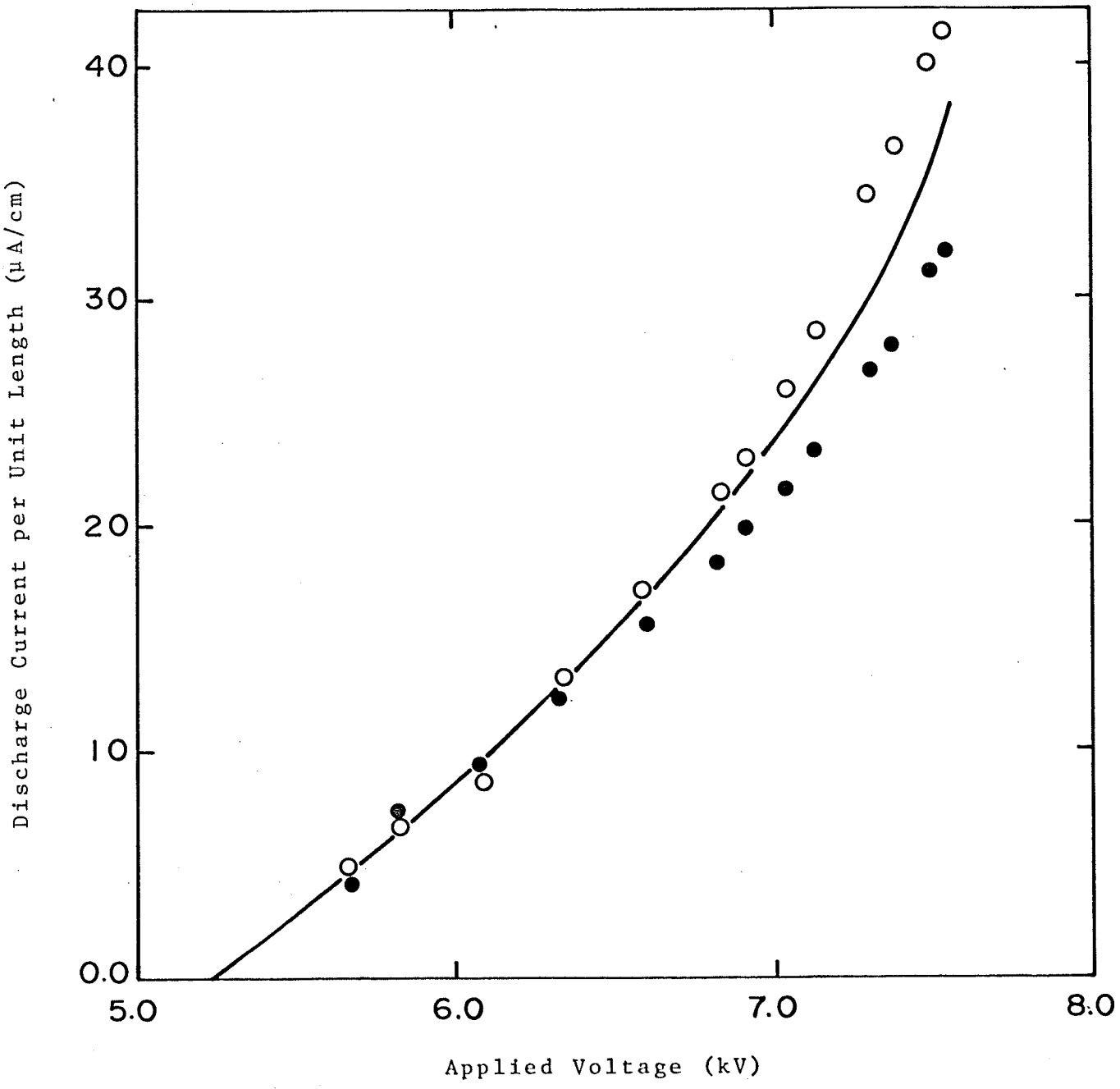
Discharge Current per Unit Length (μA/cm)
40
30
20
10
0.0
5.0
6.0
7.0
8.0
Applied Voltage (kV)

iodide concentration was independent of the radial coordinate within the errors of the measurements, and thus that the plug flow model is valid.

This result is attributed to the existence of a highly turbulent flow in the discharge tube. Since the Reynolds number is quite low (R = 20 to 80) for the conditions encountered in these experiments, this turbulence is due to the electron-ion wind[56,57]. This phenomenon is due to collisions between the neutral gas molecules flowing along the discharge tube and the negative ions and electrons being accelerated towards the discharge tube wall, and results in the methyl iodide concentration being independent of the radial coordinate. This observation has also been made in the measurement of dust concentrations in a corona discharge tube[58].

Having ascertained that the assumptions made in the Theory section of this work may be experimentally confirmed, the reaction mechanism given in reactions R1-R19 may be analyzed and compared to the experimental results. It will be useful to reintroduce this mechanism here as it will be referred to frequently in the subsequent discussion.

$$CH_3I + e \rightarrow CH_3 + I^- \quad (R1)$$

$$CH_3I + e \rightarrow CH_3 + I + e \quad (R2)$$

$$CH_3 + I \overset{M}{\rightarrow} CH_3I \quad (R3)$$

$$CH_3 + CH_3 \rightarrow C_2H_6 \quad (R4)$$

$$I + I \overset{M}{\rightarrow} I_2 \quad (R5)$$

$$CH_3 + I_2 \rightarrow CH_3I + I \quad (R6)$$

$$CH_3 + CH_3I \rightarrow CH_4 + CH_2I \quad (R7)$$

$$CH_2I + I \overset{M}{\rightarrow} CH_2I_2 \quad (R8)$$

$$CH_2I + I_2 \rightarrow CH_2I_2 + I \quad (R9)$$

$$CH_2I + CH_3 \rightarrow C_2H_5I \quad (R10)$$

$$CH_2I + CH_2I \rightarrow C_2H_4I_2 \quad (R11)$$

$$CH_3 + CH_3I \rightarrow C_2H_6 + I \quad (R12)$$

$$CH_2I + CH_3I \rightarrow CH_2I_2 + CH_3 \quad (R13)$$

$$CH_3 + CH_2I \rightarrow C_2H_4 + HI \quad (R14)$$

$$I + CH_3I \rightarrow CH_3 + I_2 \quad (R15)$$

$$I + CH_3I \rightarrow HI + CH_2I \quad (R16)$$

$$I^- \rightarrow I_{(ads)} \quad (R17)$$

$$I \rightarrow I_{(ads)} \quad (R18)$$

$$I_2 \rightarrow I_{2(ads)} \quad (R19)$$

In order to determine if the free radical chain reaction initiated by reaction R7 (in which a methyl radical abstracts an H atom from methyl iodide to form methane and an iodomethyl radical) plays an important role in determining the rate of methyl iodide decomposition, the products of the corona discharge decomposition were monitored using the mass spectrometer. If R7 was to occur at a significant rate, one would expect to see appreciable amounts of HI, CH_2I_2, C_2H_5I and $C_2H_4I_2$ formed during the methyl iodide decomposition. Furthermore, high initial concentrations of methyl iodide should enhance the rate of formation of these species, since the rate of R7 is proportional to the methyl iodide concentration. Several experiments were performed in order to determine the importance of this reaction channel.

In one set of experiments, the mass spectrometer was initially calibrated with samples of known concentration in methyl iodide and methylene iodide. It was assumed that the ionization efficiency of HI and C_2H_5I would be similar to that of CH_3I, while that of $C_2H_4I_2$ would be similar to CH_2I_2. With this assumption, it was then possible to determine the absolute concentrations of the iodo species formed during the methyl iodide decomposition.

A sample containing 500 μL/L of methyl iodide in nitrogen was allowed to flow through the discharge tube at a rate of 0.5 L/min. The mass peaks corresponding to the parent ions of $C_2H_4I_2$, C_2H_5I, CH_2I_2 and I_2 were continuously monitored while varying the discharge current. (HI^+ was not monitored as this ion is formed from all of the aforementioned organic iodides during electron impact ionization in the mass spectrometer.) In most cases, it was determined that the concentrations of these species (I_2, $C_2H_4I_2$, CH_2I_2 and C_2H_5I) were less than the lower limit of sensitivity of the mass spectrometer ($\sim$ 1 μL/L). Even under conditions which gave rise to changes in methyl iodide concentrations greater than 100 μL/L, less than 2 μL/L of the investigated iodo species were formed. This would indicate that gas phase abstraction of hydrogen from methyl iodide by methyl radicals is not a major process in the corona discharge. Two further experiments were performed which support this conclusion.

In the first of these experiments, the mass spectrometer ion lenses were adjusted in order to achieve maximum sensitivity over the range $125 \leq m/z \leq 145$. A gas stream containing 100 μL/L of methyl

iodide was allowed to flow through the discharge tube, and the peak intensity ratios $[I^+]/[CH_3I^+]$, $[HI^+]/[CH_3I^+]$, and $[CH_2I^+]/[CH_3I^+]$ were determined with no voltage applied to the discharge tube. These ratios were then monitored while varying the discharge current. Since the species HI, I_2, CH_2I_2, $C_2H_4I_2$ and C_2H_5I all have fragment ions at m/z 127, 128 and/or 141, their formation in the discharge should cause a change in the aforementioned ratios. As can be seen in Figure 12, these ratios remained constant (within experimental error) with discharge current, which gives further support to the premise that R7 is not an important reaction in the overall mechanism.

Based on these results, it was presumed that ethane would be the only organic species formed during the decomposition. This hypothesis was tested by first calibrating the mass spectrometer with a sample containing 60 μL/L of ethane in nitrogen, and subsequently monitoring the ethane (m/z 30) and methane (m/z 16) peaks when passing a gas stream containing 100 μL/L of methyl iodide through the discharge. Due to background peaks in the regions of interest (O^+ at m/z 16, $^{15}N_2^+$ and CH_2O^+ at m/z 30), there were some sensitivity limitations in detecting these species. However, it was determined that ethane appeared to be formed stoichiometrically (±10%) with the amount of methyl iodide decomposed, while the methane concentration remained below detectable levels.

On the basis of this and the previously described experiments, several reactions may be omitted from the reaction mechanisms, as they play at most a minor part in the overall processes. Specifically, since none of the products which would be associated with hydrogen abstraction

FIGURE 12 Ratio of peak intensities for the indicated ions vs the discharge current

● $[I^+]/[CH_3I^+]$

▼ $[HI^+]/[CH_3I^+]$

■ $[CH_2I^+]/CH_3I^+]$

Experimental conditions:

Initial methyl iodide concentration - 100 μL/L

Bulk gas flow rate - 1.0 L/min

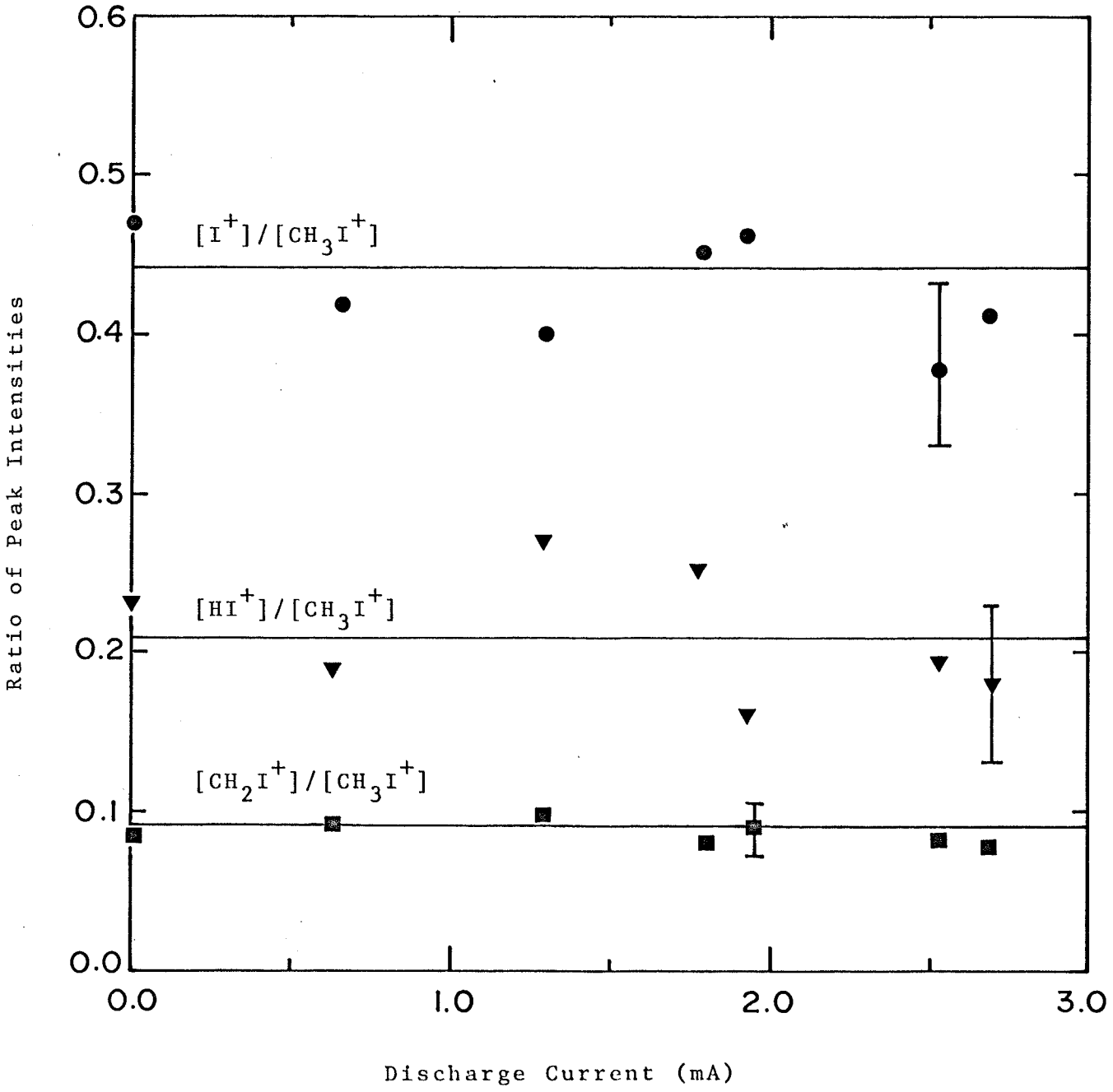
0.6
0.5
0.4
0.3
0.2
0.1
0.0
0.0
1.0
2.0
3.0
[I+]/[CH3I+]
[HI+]/[CH3I+]
[CH2I+]/[CH3I+]
Ratio of Peak Intensities
Discharge Current (mA)

by methyl radicals are observed, it may be assumed that the rate of reaction R7 is small enough that this reaction may be ignored. Since this is the only process which gives rise to iodomethyl radicals, all subsequent reactions involving CH_2I may also be deleted from the reaction scheme.

At this point, it is interesting to consider why the hydrogen abstraction reaction (R7) plays such an important role in the photolysis of methyl iodide, yet seems to have a negligible effect during the corona discharge induced decomposition of methyl iodide. In typical methyl iodide photolysis experiments, the energy of the absorbed photon is greatly in excess of the H_3C-I bond dissociation energy[59]. For a photon at 266 nm, approximately 230 kJ/mole (2.4 ev/molecule) will remain after the primary dissociation, and a large proportion of this energy will initially be concentrated in the methyl radical as translation and/or vibration[50]. In fact, it has been demonstrated that the methyl radical formed is typically vibrationally excited, predominantly in the "umbrella bending" mode[60,61]. It is this excess internal energy in the methyl radical which allows the hydrogen abstraction reaction to proceed at an appreciable rate during photolysis. The activation energy for the reaction:

$$CH_3 + CH_3I \rightarrow CH_4 + CH_2I$$

is approximately 51.7 kJ/mole[62], and thus thermal methyl radicals will abstract hydrogen very slowly ($k_{abs} \simeq 1.0 \times 10^{-30}$ $cm^3 molecule^{-1} s^{-1}$ at

300 K). However, the "hot" methyl radicals formed during photolysis may overcome this activation energy barrier quite easily.

In contrast to the photolytic decomposition of methyl iodide, the methyl radical formed during electron capture will typically have near thermal energy, as there is only 60 kJ/mole (as compared to 230 kJ/mole) excess energy in the electron capture process. If this excess energy is predominantly translational, the methyl radical will quickly be thermalized by collisions with the nitrogen molecules. Furthermore, since the highest methyl iodide concentration used in this work was 500 μL/L, a "hot" methyl radical would have to survive on the order of 2000 collisions with the carrier gas molecules before colliding with a methyl iodide molecule. (In typical photolysis experiments, the methyl iodide concentration was on the order of several percent.) In light of this, it is not overly surprising that the abstraction process plays an insignificant part in the reaction mechanism.

On the basis of kinetic data, reactions involving the abstraction of H and/or I from methyl iodide by iodine atoms (R15 and R16) may also be deleted from the mechanism. Both of these reactions have large activation energies (130 kJ/mole[63] and 80 kJ/mole[64] for H and I abstraction, respectively), and thus will be slow at 300 K.

We may now propose a somewhat simplified mechanism to govern the decomposition of methyl iodide in a corona discharge:

Reaction	Rate	
$CH_3I + e \rightarrow CH_3 + I^-$	$I_T/\pi R^2 L(1-\exp(-[CH_3I]_a \int^R \sigma_v(r)dr))$	(R1')
$CH_3I + e \rightarrow CH_3 + I + e$	$I_T/\pi R^2 L\ K[CH_3I]$	(R2')
$CH_3 + CH_3 \rightarrow C_2H_6$	$k_3[CH_3]^2$	(R3')
$CH_3 + I \xrightarrow{M} CH_3I$	$k_4[CH_3][I]$	(R4')
$CH_3 + I_2 \rightarrow CH_3I + I$	$k_5[CH_3][I_2]$	(R5')
$I + I \xrightarrow{M} I_2$	$k_6[I]^2$	(R6')
$CH_3 + CH_3I \rightarrow C_2H_6 + I$	$k_7[CH_3][CH_3I]$	(R7')
$I^- \rightarrow I_{(ads)}$	$k_{drift}[I^-]$	(R8')
$I \rightarrow I_{(ads)}$	$k_{ads}[I]$	(R9')
$I_2 \rightarrow I_{2(ads)}$	$k_{ads}[I_2]$	(R10')

where I_T is the total discharge current, $\pi R^2 L$ is the volume of the discharge tube, and the subscript (ads) indicates that the species is adsorbed on the discharge tube wall.

The rates of reactions R1' and R2' (Eqns 49 and 53, respectively) were derived previously, and contain two parameters which have yet to be determined. These are the cross section at the maximum of the electron attachment cross section function, σ_{max}, and K, which is essentially a fitting parameter related to the probability of an electron molecule interaction resulting in the cleavage of the methyl-iodine bond. The rate constants for reactions R3' to R6' are well documented in the literature, and have the following values at 300 K and 760 torr:

$$k_3 = 4.0\text{x}10^{-11}\ cm^3 molecule^{-1} s^{-1} \quad (65)$$

$$k_4 = 8.3\text{x}10^{-12}\ cm^3 molecule^{-1} s^{-1} \quad (66)$$

$$k_5 = 1.0 \times 10^{-11} \text{ cm}^3 \text{molecule}^{-1} \text{s}^{-1} \quad (67)$$

$$k_6 = 3.0 \times 10^{-13} \text{ cm}^3 \text{molecule}^{-1} \text{s}^{-1} \quad (68).$$

The rate constants for the adsorption reactions will essentially be measurements of the lifetime of these species in the discharge tube. These reactions are required in the mechanism to ensure mass balance of the iodine species, since no iodine containing products (other than CH_3I) were observed in the effluent gas from the discharge tube. In the case of reaction R8', this lifetime is determined by the mean time required for an I^- ion formed at position r in the discharge tube to drift under the influence of the electric field to the wall of the discharge tube. Since reactions R9' and R10' involve neutral species, the lifetime is not affected by the electric field. However, due to the electron/ion wind discussed previously, these reaction rates will not be diffusion-controlled, but will instead be controlled by the turbulence of the system. In effect, the rates of these reactions will be a measure of the effectiveness of the electron wind in bringing species in contact with the discharge tube surface. In subsequent analysis of experimental data, the rates of these reactions were used as fitting parameters.

Reaction R7', which involves the substitution of a methyl radical for the iodine atom in methyl iodide, has been proposed frequently in the literature[47,48,50,69]. However, no estimate of the rate for this reaction has been obtained, and thus the rate constant k_7 had to be determined from the least squares fit of the proposed mechanism to the experimental data.

Experimental data obtained related the change in concentration of methyl iodide (ΔC) to the total discharge current (I_T). This relationship was examined with flow rates ranging from 0.5 to 2.5 L/min, and initial concentrations of methyl iodide ranging from 10 to 500 μL/L. Subsequent analysis of the data was rather complicated, and thus shall be described in considerable detail.

While obtaining the ΔC-I_T data, voltage-current data were also acquired. By fitting the current-voltage data to Eqn 30, the onset voltage, V_c, was obtained. This was used in conjunction with Eqn 29 to determine the electric field in the discharge tube for any given voltage, V. The electric field thus determined was then inserted into Eqn 40, which was subsequently integrated over the radial coordinate to obtain the radially-integrated, energy-averaged cross section, in which σ_{max} remained an undetermined parameter. This was then used in Eqn 49 to determine the rate of electron attachment processes.

The reaction mechanism given in reactions R1' to R10' was then expressed as a system of simultaneous differential equations. It was determined that four equations were required to describe the rate of methyl iodide decomposition:

$$\frac{d[CH_3I]}{dt} = -\frac{I_T}{\pi R^2 L}\left(K[CH_3I]+1-\exp(-[CH_3I]\sigma'\sigma_{max})\right) - k_7[CH_3][CH_3I]$$

$$+ k_4[CH_3][I] + k_5[CH_3][I_2]$$

$$\frac{d[CH_3]}{dt} = \frac{I_T}{\pi R^2 L}(K[CH_3I]+1-\exp(-[CH_3I]\sigma'\sigma_{max})) - k_7[CH_3][CH_3I]$$

$$- k_4[CH_3][I] - k_5[CH_3][I_2] - 2k_3[CH_3]^2$$

$$\frac{d[I]}{dt} = \frac{I_T}{\pi R^2 L}(K[CH_3I]) + k_7[CH_3][CH_3I] - 2k_6[I]^2$$

$$- k_4[CH_3][I] - k_{ads}[I]$$

$$\frac{d[I_2]}{dt} = k_6[I]^2 - k_5[CH_3][I_2] - k_{ads}[I_2]$$

where σ' is the normalized energy-integrated, radially-averaged cross section[70].

A program (see Appendix) was then developed which solved this system of differential equations, subject to the boundary conditions:

At $t = 0$ $[CH_3I]$ = initial concentration of methyl iodide

$[CH_3] = 0.0$

$[I] = 0.0$

$[I_2] = 0.0$,

and calculated the final concentration of methyl iodide at a time which corresponded to the total contact time with the discharge ($t_F = \pi R^2 L(cc)/Flow(cc/s)$). The rate constants which were found in the literature (k_3-k_6) were fixed at the values stated previously. Variable parameters in the program were:

σ_{max} - the maximum of the electron attachment distribution,

K - the high energy process "rate" parameter,

k_{ads} - the rate of adsorption of iodine species at the discharge tube wall, and

k_7 - the rate of reaction between methyl radicals and methyl iodide to form ethane and I atoms.

The program utilized a non-linear, least-squares fitting routine[55] to determine the values of K, σ_{max}, k_7 and k_{ads}, which best fit the experimental data.

It was determined that the mechanism previously given provided an excellent fit to all of the experimental data (both in the stainless steel and the copper discharge tube), and determined a self-consistent set of values for the parameters, σ_{max}, K, k_{ads} and k_7. Typical data are given in Figures 13 to 16, where the solid curves were calculated from the model. The mean values of the parameters were determined to be:

$$\sigma_{max} = 186 \pm 20 \text{ Å}^2$$

$$K = (2.0 \pm 0.5) \times 10^{-16} \text{ cm}^3$$

$$k_{ads} = 5.1 \pm 1 \text{ s}^{-1}$$

$$k_7 = (2.1 \pm 0.3) \times 10^{-14} \text{ cm}^3 \text{molecule}^{-1} \text{s}^{-1}$$

where the errors quoted are the standard deviation of the mean.

FIGURE 13 Experimental data relating the change in methyl iodide concentration to the discharge current. The solid curve indicates the fit to the data based on the mechanism given in the text.

Experimental conditions:

Initial methyl iodide concentration - 25 μL/L

Bulk gas flow rate - 1.0 L/min

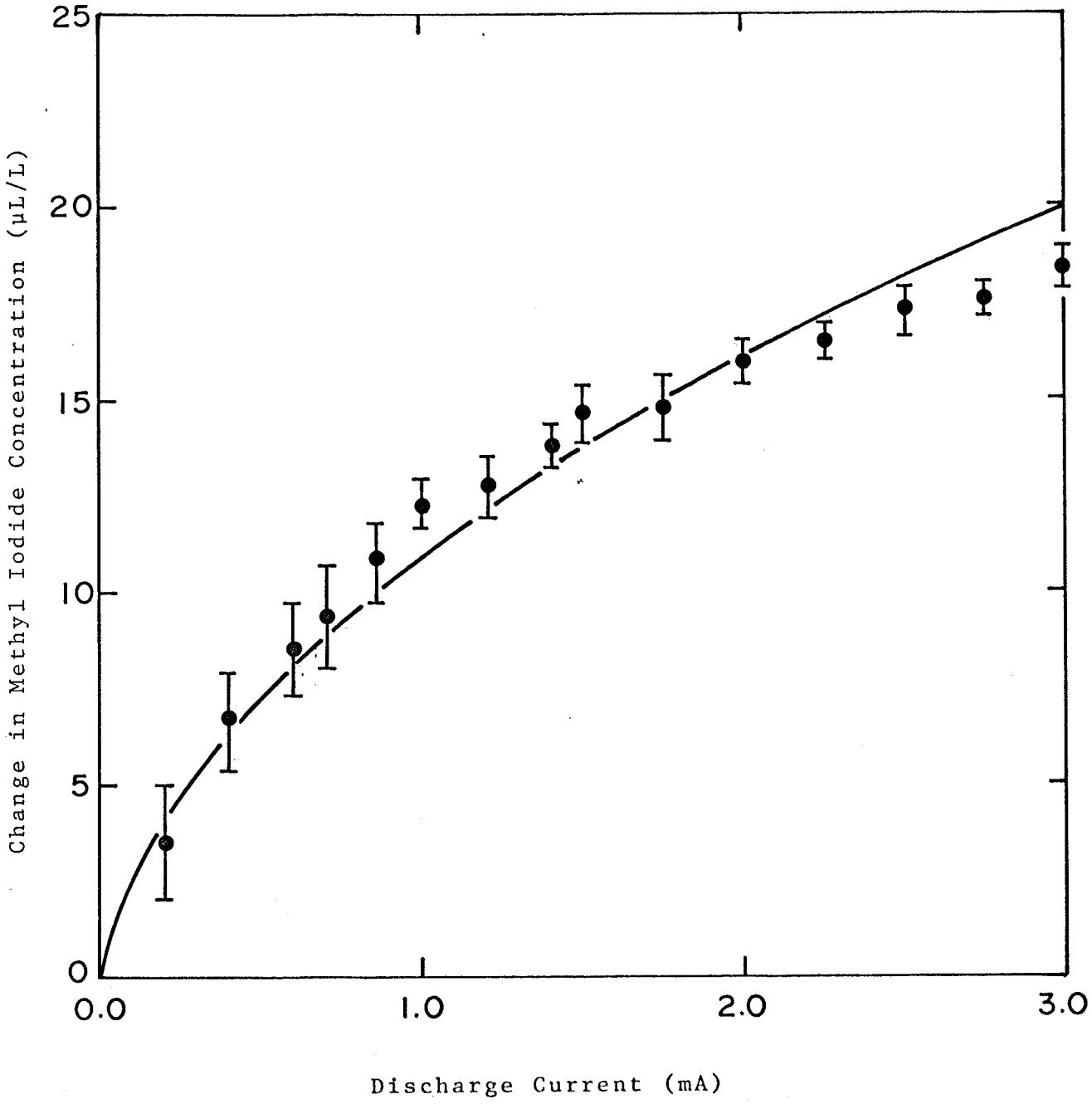
25
20
15
10
5
0
0.0
1.0
2.0
3.0
Change in Methyl Iodide Concentration (µL/L)
Discharge Current (mA)

FIGURE 14 Experimental data relating the change in methyl iodide concentration to the discharge current. The solid curve indicates the fit to the data based on the mechanism given in the text.

Experimental conditions:

Initial methyl iodide concentration - 53 μL/L

Bulk gas flow rate - 2.0 L/min

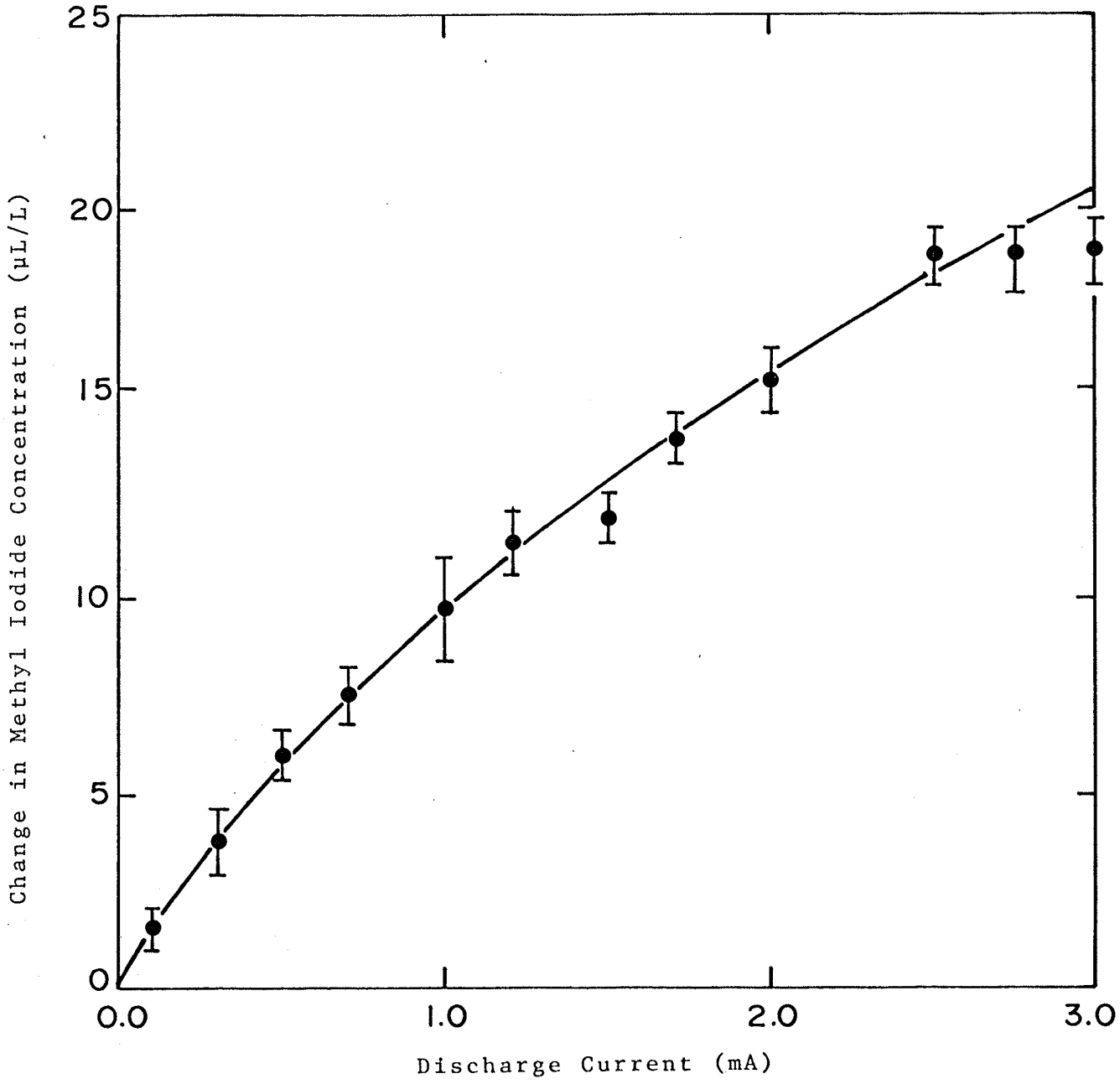
25
20
15
10
5
0
0.0
1.0
2.0
3.0
Change in Methyl Iodide Concentration (µL/L)
Discharge Current (mA)

FIGURE 15 Experimental data relating the change in methyl iodide concentration to the discharge current. The solid curve indicates the fit to the data based on the mechanism given in the text.

Experimental conditions:

Initial methyl iodide concentration - 100 μL/L

Bulk gas flow rate - 0.75 L/min

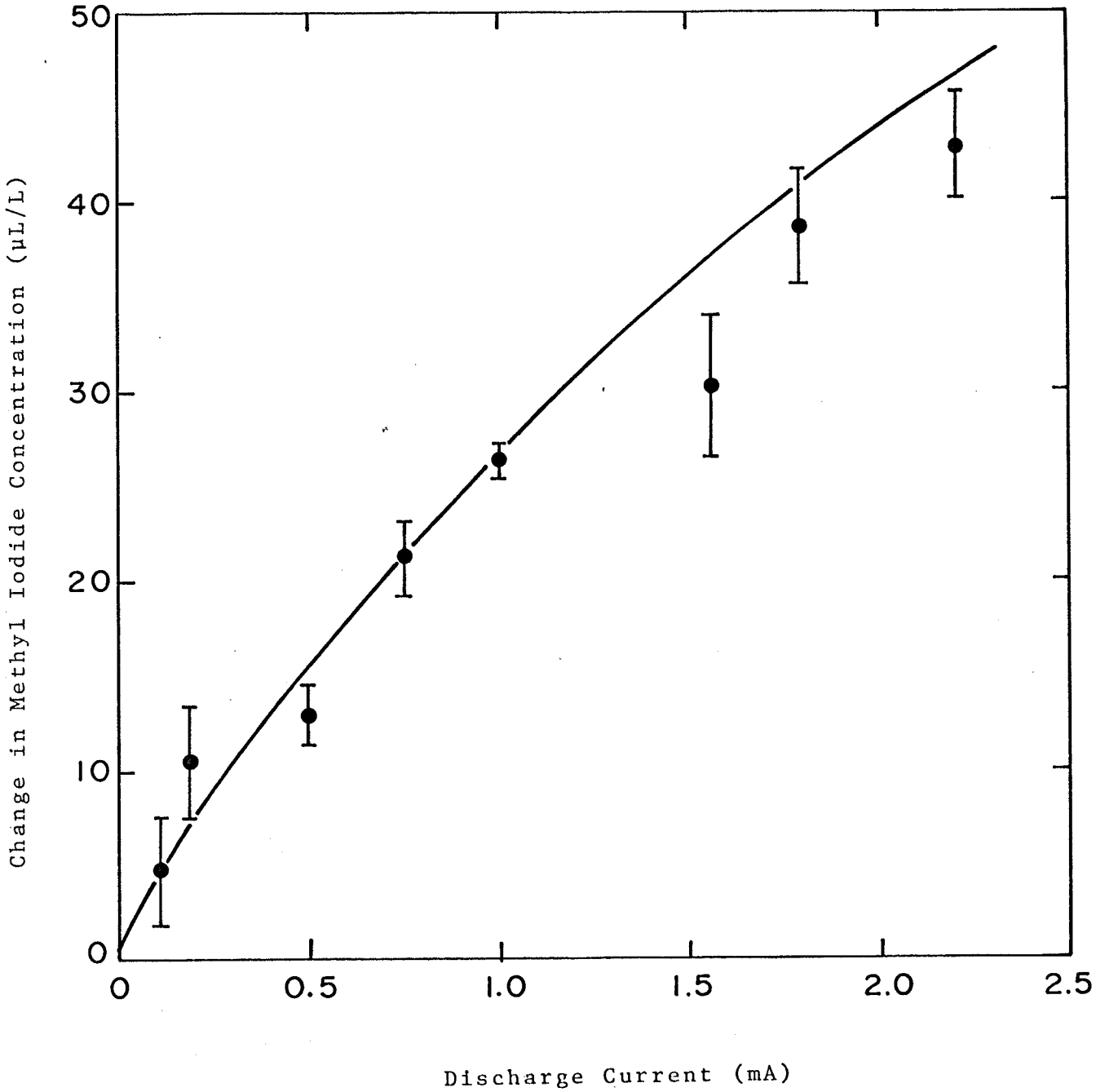
Change in Methyl Iodide Concentration (µL/L)
50
40
30
20
10
0
0
0.5
1.0
1.5
2.0
2.5
Discharge Current (mA)

FIGURE 16 Experimental data relating the change in methyl iodide concentration to the discharge current. The solid curve indicates the fit to the data based on the mechanism given in the text.

Experimental conditions:

Initial methyl iodide concentration - 500 μL/L

Bulk gas flow rate - 0.5 L/min

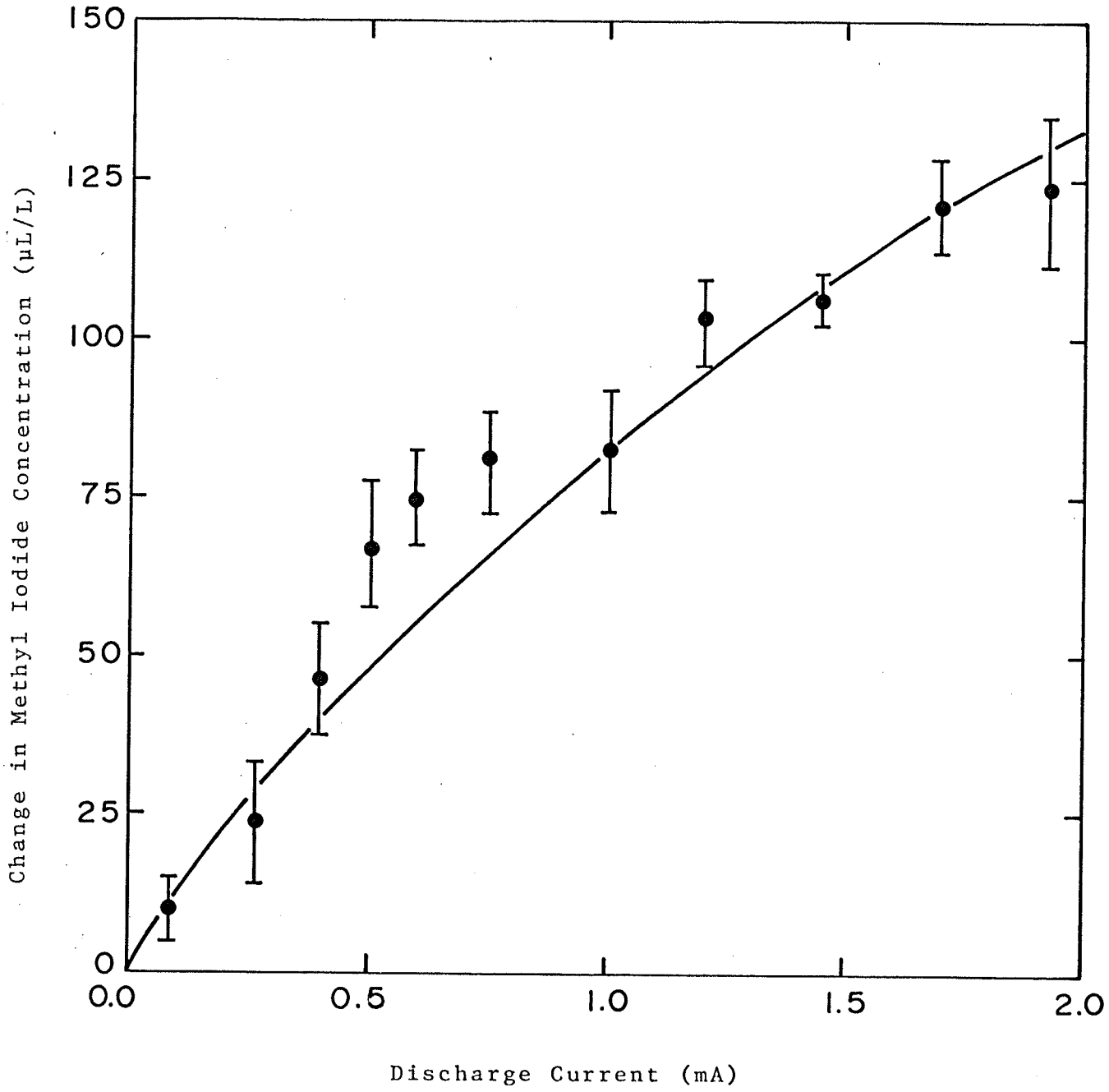
150
125
100
75
50
25
0
0.0
0.5
1.0
1.5
2.0
Change in Methyl Iodide Concentration (µL/L)
Discharge Current (mA)

The value determined for σ_{max} indicates that the cross section for electron attachment to methyl iodide is quite large, as was expected qualitatively from previous investigations[40,47,71-73]. It should be noted that this is the cross section at the resonance energy, i.e. the cross section at the maximum of the electron attachment function. Although no previous values of the maximum cross section for CH_3I are to be found in the literature, a cross section of the magnitude determined in this work is comparable to that determined for other electron-attaching species. For example, the maximum cross section for electron capture by HI is approximately 200 $Å^2$[74], while that of CCl_4 is on the order of 1000 $Å^2$[75].

Unfortunately, the magnitude of the radially-integrated, energy-averaged, high-energy cross section (as defined in Eqn 53) cannot be compared to any previous data, as it is not certain which reaction channels K encompasses.

Possible reaction channels for these processes include the electronic excitation of methyl iodide to a dissociative state:

$$CH_3I + e \xrightarrow{M} CH_3I^* + e \quad \begin{cases} \rightarrow CH_3I \\ \rightarrow CH_3 + I \end{cases} ,$$

or the interaction of short-lived excited nitrogen molecules with methyl iodide, which may lead to dissociation:

$$N_2 + e \rightarrow N_2^* + e$$
$$N_2^* + CH_3I \rightarrow CH_3 + I + N_2 \quad .$$

Either or both of these reaction channels may be occurring in the ionization sheath.

The rates for the adsorption processes were determined to be 5.1 s^{-1}, which corresponds to a "wind velocity" on the order of 10 cm s^{-1}. Although no information in the literature exists on the ion wind velocity in a cylindrical corona discharge tube, this velocity has been measured in point-to-plane discharges[56,57], and was found to be on the order of 1 m s^{-1}. However, this discharge geometry (point-to-plane) gives rise to a more localized discharge and much higher ion densities than a coaxial cylinder discharge. Thus, an ion wind velocity on the order of 10 cm s^{-1} is certainly not unreasonable for the cylindrical corona discharge tube.

Methyl radicals were found to react with methyl iodide to give ethane and iodine, with a rate constant of $(2.0\pm0.3)\times10^{-14}$ $cm^3 molecule^{-1} s^{-1}$. As mentioned previously, the rate of this process has not been previously measured, nor has a detailed reaction mechanism been proposed. Owing to the magnitude of this rate constant, the activation energy for this reaction must be reasonably small ($E_a \lesssim 20$ kJ/mole). Since the reaction is exothermic by $\sim$ 30 kJ/mole, it is not a thermodynamically unfavourable process.

A possible mechanism which may account for this process involves a transition state complex of the form CH_3ICH_3[50] (see Figure 17), which is reasonably long-lived. The methyl radicals are only weakly bound to the iodine, and may be mobile in terms of the C-I-C bond angle. It is conceivable that the methyl radicals may then become close enough that reaction may occur. A similar process to this has been postulated to explain the non-Arrhenius behaviour of the reaction:

$$HI + F \rightarrow HF + I \quad , \qquad (R11')$$

which has been observed to proceed faster at low temperatures than would be expected from the high temperature data. Wurzberg et al.[76,77] have proposed that this reaction proceeds directly through abstraction of hydrogen by the fluorine atom at high temperatures, while at low temperatures, an activated complex of the form H-I-F is produced, which subsequently disproportionates via the same mechanism as that predicted for the CH_3-I-CH_3 complex, to form HF. In light of this, it is not unreasonable to predict that R7' proceeds via this mechanism, although it may be impeded by steric hindrance.

SUMMARY AND CONCLUSIONS

Equations have been derived that describe the electric field in a corona discharge tube (in the presence of electron-attaching species), accurately predict the current-voltage characteristics of the tube, and allow the determination of ionic mobilities from current-voltage data.

FIGURE 17 An activated complex for CH_3ICH_3, which may allow for variations in C-I-C bond angle.

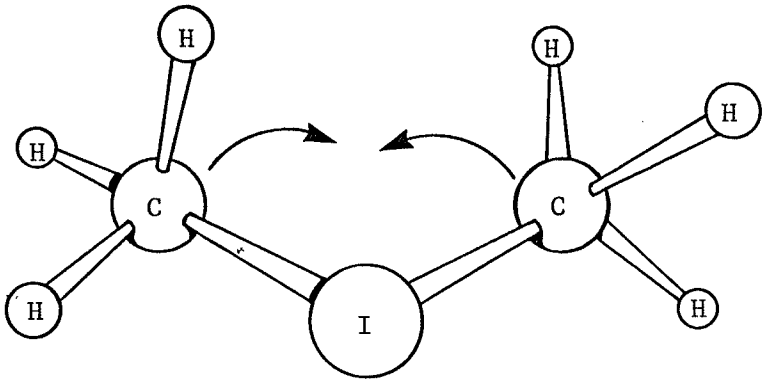
H
H
C
H
I
H
C
H
H

The electric field was used to determine the radially-averaged, energy-integrated, velocity-weighted electron attachment cross section for methyl iodide, through the evaluation of a convolution integral involving an electron attachment function and the Druyvesten energy distribution. This led to the derivation of an expression which predicts the rate of methyl iodide decomposition due to electron capture in a corona discharge. Furthermore, subsequent calculations indicated that the rate of processes occurring in the ionization sheath would vary in a linear fashion with the discharge current.

The results presented in this work lend credence to the proposal put forth previously[12,15,16], i.e. negative corona discharges may provide a convenient means for promoting the reaction and decomposition of electrophilic molecules. Although further investigation is required, it is expected that other impurities which form stable negative ions (such as NO, SO_2) will behave similarly to methyl iodide, and thus it may prove possible to scrub these species by reaction chains initiated in an electric discharge.

On the basis of the experimental results, the reaction mechanism given by reactions R1'-R10' has been shown to fit the decomposition data over the ranges of flow rate (0.5-2.5 L/min), initial concentration (10-500 μL/L), and discharge current (0-3 mA) investigated. Through the use of a non-linear, least-squares fitting routine, the following parameters have been determined:

σ_{max} - the cross section for electron attachment at the resonant energy,

K - a radially-integrated, energy-averaged, velocity-weighted cross section for decomposition of MeI in the discharge zone,

k_{ads} - the rate of iodine adsorption from the gas phase onto the walls of the discharge tube, and

k_7 - the rate of reaction between methyl radicals and methyl iodide.

The values of these parameters have been determined to be:

$$\sigma_{max} = 186 \pm 20 \text{ Å}^2$$

$$K = (2.0 \pm 0.5) \times 10^{-16} \text{ cm}^3$$

$$k_{ads} = 5.1 \pm 1.0 \text{ s}^{-1}$$

$$k_7 = (2.1 \pm 0.3) \times 10^{-14} \text{ cm}^3 \text{molecule}^{-1} \text{s}^{-1}$$

at 300 K and 760 torr N_2.

Thus, it was possible to explain the observed decomposition of methyl iodide in a corona discharge tube by elucidating some of the fundamental physical and chemical phenomena occurring.

Although the methods of analysis used are inherently complicated, the techniques described in this work may prove applicable to describing the effects of a corona discharge on other gas mixtures.

REFERENCES

1. Christophorou, L.G. and Compton, R.N., Health Phys. 13 (1967) 1277.
2. Klots, C.E. and Compton, R.N., Chem. Phys. Lett. 73 (1980) 589.
3. Kornblueh, I.H., Bull. Am. Meteor. Soc. 41 (1960) 361.
4. Watson, W.D., Rev. Mod. Phys. 48 (1976) 513.
5. Coburn, J.W., Plasma Chem. Plasma Process. 1 (1981) 319.
6. Hill, R.M. and Rhodes, C.K., Principles of Laser Plasmas, G. Bekefi (Ed.), Wiley, New York (1976).
7. Stockdale, J.A., Hurst, G.S. and Christophorou, L.G., Nature, Lond. 202 (1964) 459.
8. Bradbury, N.E., Phys. Rev. 44 (1938) 44.
9. Bortner, T.E. and Hurst, G.S., Health Phys. 1 (1958) 39.
10. Marmet, P. and Kerwin, L., Can. J. Phys. 38 (1960) 767.
11. Christophorou, L.G., Compton, R.N., Hurst, G.S. and Reinhardt, P.W., J. Chem. Phys. 43 (1965) 4273.
12. Torgerson, D.F. and Smith, I.M., Proc. 15th DOE Nuclear Air Cleaning Conference, CONF 780819 (1980) 43.
13. Smith, D. and Adams, N.G., Pure and App. Chem. 56 (1984) 125.
14. Hoenig, S.A., Sill, G.T., Kelley L.M. and Garvey, K.J., J. Air Poll. Cont. Assoc. 30 (1980) 277.
15. Kipp, E.B., Shelstad, K.A. and Castle G.S.P., Can. J. Chem. Eng. 51 (1973) 494.
16. Dickson, L.W., Torgerson, D.F. and Toft, A., 6th Int. Symp. Plasma Chem. (1983) 357.
17. Torgerson, D.F. and Smith, I.M., "Off-Gas Control Project", Atomic Energy of Canada Limited Report, AECL-5979 (1978).
18. Goldman, M. and Goldman, A., Gaseous Electronics Vol. 1, M.N. Husk and H.J. Oksam (Eds.), Academic Press, New York (1978).
19. Brown, E.C., Introduction to Electrical Discharges in Gases, John Wiley and Sons, New York (1966).
20. Loeb, L.B., Electrical Coronas, Univ. of California Press, Berkeley (1965).

21. Perkins, J.R., ASTM Spec. Tech. Pub. Eng. Diel. Vol. 1 (1979).

22. Bandel, H.W., Phys. Rev. 84 (1951) 92.

23. Llewellyn Jones, F., The Glow Discharge, John Wiley and Sons, New York (1966).

24. Townsend, J.S., Electricity in Gases, Oxford Univ. Press, London (1914).

25. Meek, J.M. and Craggs, J.D., Electrical Breakdown of Gases, John Wiley and Sons, Chuchester (1978).

26. Morrison, R.D. and Hopstock, D.M., Journal of Electrostatics 6 (1973) 349.

27. Townsend, J.S., Phil. Mag. 28 (1914) 83.

28. Cooperman, P. Trans. AIEE 79 (1960) 47.

29. Von Engl, A., Ionized Gases, Oxford Univ. Press, London (1965).

30. Sokolov, A.G., Elect. Technol. USSR 2 (1972) 28.

31. Fuje, T. and Meisels, G.G., J. Chem. Phys. 75 (1981) 5067.

32. McDaniel, E.W. and Mason, E.A., The Mobility and Diffusion of Ions in Gases, Wiley, New York (1973).

33. Thackston, M.G., Eiselle, F.L., Ellis, H.W. and McDaniel, E.W., J. Chem. Phys. 67 (1977) 1267.

34. Tikhodejev, N.N., Letters to Jour. Tech. Phys. (USSR) 1 (1975) 497.

35. Frances, G., Ionization Phenomena in Gases, Buttersworth Scientific Publication (1960).

36. Allis, W.P., in Handbuck der Physik 21, Heidelberg Springer (1956).

37. Chapman, S. and Cowling T.G., The Mathematical Theory of Non-Uniform Gases, Cambridge Univ. Press (1952).

38. Druyvesten, M.J., Physica 10 (1930) 292.

39. Loeb, L.B., Basic Processes of Gaseous Electronics, Univ. of California Press, Berkeley (1955).

40. Blaunstein, R.P. and Christophorou, L.G., J. Chem. Phys. 49 (1968) 1526.

41. Christophorou, L.G., Chaney, E.L. and Christoulides, A.A., Chem. Phys. Lett. 3 (1969) 363.

42. Careleton, N.P. and Megill, L.R., Phys. Rev. 126 (1962) 2089.

43. Dutton, J., J. Phys. Chem. Ref. Data 4 (1975),
43a, Crompton et al. in Proc. 6th Int. Conf. Ion Phen. in Gases, Hubert, P. and Cremieu-Alcan (Eds.) Vol. 1 (1963) 337.
43b, Jory, Austr. J. Phys. 18 (1965) 237.
43c, Townsend et al., Phil. Mag. 42 (1921) 874.
43d, Naidu et al., Brit. S. App. Phys. 1 (1968) 763.

44. Kerr, J.A., Chem. Rev. 66 (1966) 465.

45. Rosenstock, H.M., Draxe, K., Steiner, B.W. and Herron, J.T., J. Phys. Chem. Ref. Data 6, supp. #1 (1977).

46. Wright, A.N. and Winkler, C.A., Active Nitrogen, Academic Press, New York (1968).

47. Stockdale, J.A., Davis, F.J., Compton, R.N. and Klots, C.E., J. Chem. Phys. 60 (1974) 4270.

48. Gradshteyn, I.M. and Ryzkik, I.M., Tables of Integrals, Series and Products, Academic Press, New York (1980).

49. Lawrence, F.S. and Allen, R.C., Numerical Computing, W.B. Saunders Co., Philadelphia (1973).

50. Majer, J.R. and Simons, J.P., Adv. in Photochemistry, Vol. 2 (1964) 127.

51. Schuler, H.R. and Chiniel, C.T., J. Am. Chem. Soc. 75 (1953) 3792.

52. Petry, R.C. and Schuler, H.R., J. Am. Chem. Soc. 75 (1953) 3796.

53. Rebbert, R.E. and Ausloos, P., J. Chem. Phys. 48 (1968) 306.

54. Wren, D.J. and Vikis, A.C., J. Chem. Thermo. 14 (1982) 435.

55. Bevington, P.R., Data Reduction and Error Analysis for the Physical Sciences, McGraw Hill (1969).

56. Hoenig, S.A., Conf. Rec. IAS Ann. Mtg. (IEEE) 2 (1980) 1032.

57. Hoenig, S.A., Conf Proc. 4th Int. Symp. Plasma Chem. (1979) 617.

58. Mirzabeykan, G.Z. and Grigor'ev, I.N., Electr. Technol. USSR 3 (1972) 59.

59. Schultz, R.D. and Taylor, H.A., J. Chem. Phys. 18 (1950) 194.

60. Shapiro, M. and Bersohn, R., J. Chem. Phys. 73 (1980) 3810.

61. Sparks, R.K., Shobatake, K., Carlson, L.R. and Lee, Y.T., J. Chem. Phys. 75 (1981) 3838.

62. Skinner, G.B. and Ringrose, G.H., J. Chem. Phys. 43 (1965) 429.

63. Furuyama, S., Golden, D.M. and Denson, S.W., Int. J. Chem. Kinet. 1 (1969) 283.

64. Flowers, M.C. and Benson, S.W., J. Chem. Phys. 38 (1963) 882.

65. Baulch, B.L. and Duxbury, J., Comb. and Flame 37 (1980) 313.

66. This rate constant has been assumed to be the same as that for $CF_3 + I \rightarrow CF_3I$. Skorobagatov, G.A., Seleznev, V.G. and Slesar, O.N., Dokl. Akad. Nauk SSSR, Ser. Khim. 231 (1976) 1407 (Russian), 231 (1976) 1292 (English).

67. Christie, M.I., Proc. Roy. Soc. London Serv. A 244 (1958) 411.

68. Ip, J.K.K. and Burns, G., J. Chem. Phys. 51 (1972) 3414.

69. Souffil, R.D., Hamill, W.H. and Williams, R.R., J. Am. Chem. Soc. 78 (1956) 917.

70. This was evaluated by integrating Eqn 40 over r, while considering the maximum attachment cross section to be 1 $Å^2$.

71. Wentworth, W.E., Becker, R.B. and Tung, R., J. Phys. Chem. 71 (1967) 1652.

72. Spence, D. and Schulz, G.J., J. Chem. Phys. 58 (1973) 1800.

73. Wentworth, W.E., George, R. and Keith, H., J. Chem. Phys. 51 (1969) 1791.

74. Christophorou, L.G. and Compton, R.N., Health Phys. 13 (1967) 1277.

75. Christoulides, A.A. and Christophorou, L.G., J. Chem. Phys. 54 (1971) 4691.

76. Wurzberg, E. and Houston, P.L., J. Chem. Phys. 72 (1980) 5915.

77. Wurzberg, E., Grimley, A.J. and Houston, P.L., Chem. Phys. Lett. 57 (1978) 373.

APPENDIX

Data analysis was performed in two separate programs. The first of these (program CAPTUR) calculated the onset voltage of the discharge and the mean ionic mobility by fitting current voltage data to Eqn 30 through the use of CHIFIT[1], a non-linear least squares routine. CAPTUR also evaluated the radially-averaged, energy-integrated electron attachment cross section by numerically[2] evaluating the radial integral of Eqn 49.

The second program (FIT) utilized a subroutine (STIFFZ[3]) to solve the system of differential equations which defined the reaction scheme (eqns given on pages 67-68). CHIFIT was again used to determine the rate constants which gave best agreement with the experimental data.

Programs FIT and CAPTUR are presented here to illustrate the methods used in data analysis.

1. Bevington, P.R., Data Reduction and Error Analysis for the Physical Sciences, McGraw Hill (1969).

2. Lawrence, F.S. and Allen, R.C., Numerical Computing, W.B. Saunders Co., Philadelphia (1973).

3. Carver, M.B. and McEwan, S.R., "Simulation of an Implicitly Defined Differential Equation System Subject to Numerous Discontinuities", Applied Mathematical Modelling (1978).

```
      PROGRAM CAPTUR
C
C     PURPOSE
C             analyze experimental data related to the corona discharge
C             decomposition of methyl iodide.
C
C     Noteworthy parameters
C
C     Sigmax  -maximum of the electron attachment function
C     Curr    -array of values for the discharge current
C     Volt    -array of values for the voltage
C     Df      -array fo values for the decontamination factors
C     A       -array of values for fitting parameters
C     Sigmaa  -array of standard deviations in A
C     Deltaa  -array of increments for A
C     Fn      -1.le.n.le.6 results of numerical integration
C     Ans     -array of values of convolution integrals
C     Cons    -square of elcectric field at point where fit changes
C     Rn      -radius at which the fit changes
C
C     Functions called
C
C     F       -function to be integrated to calculate the first part
C              of the convolution
C     G       -function to be integrated to calculate the second part
C              of the convolution
C     Fchisq  -calculates the rdeuced chi-squared for data and fit
C     Functn  -calculates the value of the fitting function for given
C              value of the independant parameter
C
C     Subroutines called
C
C     Spacc   -calculates the space charge contribution to the electric
C              field
C
C     Chifit  -performs a non-linear least squares fit to data by
C              parabolic extrapolation of chi square
C
C     Matinv  -inverts a symmetric square matrix, and calculates the
C              determinant
C
C     Integ   -numerically integrates a function by Simpson's rule
C
C     NOTE    -Dimension statements in this program are valid for
C              up to 40 data points,and two fitting parameters
C
      EXTERNAL F,G,FCHISQ,FUNCTN
      INTEGER SIGMAX,SYGMAX
      DIMENSION CURR(40),VOLT(40),DF(40),ANS(40),A(2),V(10),VCALC(10)
      DIMENSION SPACE(40),DELTAA(2),SIGMAY(40),YFIT(40),SIGMAA(2)
      DOUBLE PRECISION FCHISQ,CHISQR
      LOGICAL SWT
      LOGICAL*1 FNAM(20),TITLE(80)
C
C     REQUESTS GLOBAL PARAMETERS
C
      TYPE 35
   35 FORMAT(' MAXIMUM CROSSECTION(I4,ANG**2)=',$)
      ACCEPT 15,SIGMAX
   15 FORMAT(I4)
      SYGMAX=SIGMAX
  601 TYPE 599
  599 FORMAT(' ESTIMATE OF MEAN MOBILITY=',$)
```

```
      ACCEPT 5,A(1)
    5 FORMAT(F5.2)
      A(2)=5.0
      MODE=0.0
      DELTAA(1)=0.05*A(1)
      DELTAA(2)=0.05
      NTERMS=2
C     This section of the program reads data from a file
C     with structure:
C
C     Title(80 characters)
C     ACC,A1,B1
C     NPTS,ICONC,FLOW
C     CURR(1),VOLT(1),DF(1)
C     CURR(2),....
C
C     ACC-Required accuracy of integrals(usually 1.0E-06) E10.3
C     A1-Radius of the filament in cm. E10.3
C     B1-Radius of the discharge tube in cm. E10.3
C     NPTS-Number of data points I2
C     ICONC-Initial concentration of methyl iodide in uL/L I3
C     FLOW-Flow rate in cc./min F5.0
      FNAM(20)=0
      TYPE 605
  605 FORMAT(' ENTER DATAFILE NAME(dev:filnam.ext)-',$)
      ACCEPT 615,FNAM
  615 FORMAT(20A1)
      GO TO 617
  616 TYPE 606
  606 FORMAT(/,' PROGRAM TERMINTATED',/)
      STOP
  617 OPEN(UNIT=4,NAME=FNAM,TYPE='OLD',ERR=616)
  625 READ(4,630) TITLE
  630 FORMAT(80A1)
      READ(4,10) ACC,A1,B1
   10 FORMAT(3E10.3)
      READ(4,20) NPTS,ICONC,FLOW
   20 FORMAT(' ',I2,X,I3,X,F5.0)
      DO 30 I=1,NPTS
      READ(4,25,END=31) CURR(I),VOLT(I),DF(I)
      TYPE 25,CURR(I),VOLT(I),DF(I)
   25 FORMAT(3F8.3)
   30 CONTINUE
   31 CLOSE(UNIT=4)
      DO 40 I=1,NPTS
   40 SIGMAY(I)=0.0
C     SORTING ROUTINE

      N=NPTS-1
      DO 100 I=1,N
      SWT=.FALSE.
      DO 90 J=1,N
      IF(VOLT(J).LE.VOLT(J+1))GO TO 90
      TEMP=VOLT(J)
      VOLT(J)=VOLT(J+1)
      VOLT(J+1)=TEMP
      TEMP=CURR(J)
      CURR(J)=CURR(J+1)
      CURR(J+1)=TEMP
      TEMP=DF(J)
      DF(J)=DF(J+1)
      DF(J+1)=TEMP
      SWT=.TRUE.
```

```
 90     CONTINUE
        IF(.NOT.SWT)GO TO 110
100     N=N-1
110     CONTINUE
C
C       PRINT OUT DATA
C
        TYPE 120,FLOW
120     FORMAT(' FLOW RATE=',F5.0,' CC/MIN')
        TYPE 130,ICONC
130     FORMAT(' INITIAL CONCENTRATION=',I3,'UL/L')
        TYPE 140,SIGMAX
140     FORMAT(' MAXIMUM CROSSECTION=',I4,' X1E+16CM**2')
        TYPE 150
150     FORMAT(' I',4X,'CURRENT',5X,'VOLTAGE',5X,'DECONTAMINATION')
        TYPE 160
160     FORMAT(' ',4X,'(MILLIAMPS)',1X,'(KILOVOLTS)',7X,'FACTOR')
        TYPE 170
170      FORMAT(' ')
        DO 210 I=1,NPTS
        TYPE 200,I,CURR(I),VOLT(I),DF(I)
200     FORMAT(' ',I2,5X,F8.3,7X,F8.3,11X,F8.3)
210     CONTINUE
C
C       FIT CURRENT-VOLTAGE DATA TO FUNCTN
C
        M=1
205     CALL CHIFIT(VOLT,CURR,SIGMAY,NPTS,NTERMS,MODE,A,DELTAA,SIGMAA,
     1  YFIT,CHISQR)
        M=M+1
        IF(M.EQ.2) GO TO 205
        TYPE 300,A(1),SIGMAA(1)
300     FORMAT(' MEAN IONIC MOBILITY=',F6.3,' +/-',E10.3)
        TYPE 310,A(2),SIGMAA(2)
310     FORMAT(' ONSET VOLTAGE=',F6.3,' +/-',E10.3)
        TYPE 311,CHISQR
311     FORMAT(' REDUCED CHI SQUARE=',E10.3)
        VMAX=VOLT(NPTS)
        DELV=(VMAX-A(2))/10.0
        DO 314 I=1,10
        V(I)=A(2)+I*DELV
314     CONTINUE
        DO 315 I=1,10
        M=I
        VCALC(I)=FUNCTN(V,M,A)
        TYPE 320,V(I),VCALC(I)
320     FORMAT(' VOLTAGE=',F5.2,' CALCULATED CURRENT=',F8.6)
315     CONTINUE
        VC=A(2)
C
C       CALCULATES THE VALUE OF THE REQUIRED NUMERICAL INTEGRAL FOR EACH VALUE
C       OF VOLT(I). FORMS ARRAYS ANS(I) AND ERROR(I) WHICH ARE THE ESTIMATED
C       VALUE  AND THE ESTIMATED ERROR OF THE INTEGRAL FOR VOLT(I).
C
        VC=1000.*VC
        DO 400 I=1,NPTS
        VOL=VOLT(I)*1000.
        STAT=(VC/ALOG(B1/A1))**2
        CALL SPACC(VOL,VC,B1,A1,STAT,SPAC)
        SPACE(I)=SPAC
        CONS=5.108E08
        CONS2=1.63E06
        R1=(STAT/(CONS-SPAC))**0.5
```

```
      D1=3.09E-02
      D2=-2.360
      CALL INTEG(F,A1,R1,ACC,AN,ERROR,AREA,IFLAG,SPAC,STAT,D1,D2)
      IF(IFLAG.EQ.1) GO TO 355
      TYPE 354,IFLAG
354   FORMAT(' FLAG=',I1)
355   F1=AN
      CALL INTEG(G,A1,R1,ACC,AN,ERROR,AREA,IFLAG,SPAC,STAT,D1,D2)
      IF(IFLAG.EQ.1) GO TO 365
      TYPE 354,IFLAG
365   F2=AN
      IF(SPAC.GE.CONS2) GO TO 366
      R2=(STAT/(CONS2-SPAC))**0.5
      IF(R2.GE.1.9) GO TO 366
      GO TO 367
366   R2=B1
367   D1=1.185E-02
      D2=4.94E-01
      CALL INTEG(F,R1,R2,ACC,AN,ERROR,AREA,IFLAG,SPAC,STAT,D1,D2)
      IF(IFLAG.EQ.1) GO TO 375
      TYPE 354,IFLAG
375   F3=AN
      CALL INTEG(G,R1,R2,ACC,AN,ERROR,AREA,IFLAG,SPAC,STAT,D1,D2)
      IF(IFLAG.EQ.1) GO TO 385
      TYPE 354,IFLAG
385   F4=AN
      D1=2.603E-02
      D2=5.025E-02
      CALL INTEG(F,R2,B1,ACC,AN,ERROR,AREA,IFLAG,SPAC,STAT,D1,D2)
      IF(IFLAG.EQ.1) GO TO 386
      TYPE 354,IFLAG
386   F5=AN
      CALL INTEG(G,R2,B1,ACC,AN,ERROR,AREA,IFLAG,SPAC,STAT,D1,D2)
      IF(IFLAG.EQ.1) GO TO 387
      TYPE 354,IFLAG
387   F6=AN
      ANS(I)=F1+F3+F5+5.09*(F2+F4+F6)
400   CONTINUE
432   SIGMAX=SYGMAX
      TYPE 20,NPTS,ICONC,FLOW
446   DO 500 I=1,NPTS
      FCONC=ICONC/DF(I)
460   ALPHA=8.865E-19*SIGMAX*ANS(I)*2.413E+13
      TYPE 520,CURR(I),ALPHA,FCONC
500   CONTINUE
      GO TO 601
520   FORMAT(' ',2X,F5.2,3X,F7.5,3X,F6.2)
      END
      FUNCTION F(X,SPAC,STAT,D1,D2)
      S1=SPAC
      S2=STAT
      F=1/((D1*(S1+S2/X**2)**0.25+D2)**2+1.775E-02)
      RETURN
      END
      FUNCTION G(X,SPAC,STAT,D1,D2)
      S1=SPAC
      S2=STAT
      G=(D1*(S1+S2/X**2)**0.25+D2)/
     1 ((D1*(S1+S2/X**2)**0.25+D2)**2+1.775E-02)**1.5
      RETURN
      END
C
C
```

```
C
      SUBROUTINE SPACC(V,VC,B,A,STAT,SPAC)
      X1=(V/VC-1)*ALOG(B/A)+1.6931
      ROOT=(X1+15)*(X1-1)
      QUAD=((X1-3+SQRT(ROOT))/2)**2-1
      SPAC=STAT*QUAD/B**2
      RETURN
      END
```

```
FIT,B0919-10270,T500.     HARRIS
FTN(R=2)
LGO.
/*EOR
      PROGRAM FIT(INPUT,OUTPUT,TAPE5=INPUT,TAPE6=OUTPUT)
      DIMENSION Y(4),WS(62),XD(30),YD(30),SIGMAY(30),A(4),
     1  SIGMAA(4),YFIT(30),S(30),DELTAA(4),AB(4)
      DIMENSION ALPHA(4,4),BETA(4),DA(4),ALPH(4,4)
      COMMON/STAT/KOUNT(7)
      COMMON/XTZQ/YO,FLO,A,CURR,CROSS,R1,R2,R3
      EXTERNAL EQNSF,FCHISQ
C     THISPROGRAM SOLVES THE STIFF DIFFERENTIAL EQUATIONS DESCRIBING THE
C     DECOMPOSITION OF METHYL IODIDE IN A NITROGEN CORONA DISCHARGE.
C     ***REACTIONS***                ***RATE***
C     CH3I+E=CH3+I+E          0.4956*CURR*(1-EXP(-S*CH3I))
C     CH3I+E=CH3+I-              0.4956*CURR*R*CH3I
C     CH3+CH3=C2H6                 R2*(CH3)**2
C     I+I=I2                        R3*(I)**2
C     CH3+I=CH3I                    R1*CH3*I
C     CH3+I2=CH3I+I                 R1*CH3*I2
C     I=I(WALL)                       R7*I
C     I2=I2(WALL)                     R8*I2
C     CH3+CH3I=C2H6+I              R10*CH3*CH3I
C
C     A NON-LINEAR LEAST SQUARES FIT TO THE SOLUTION OF THE D.E.'S IS
C     PROVIDED BY PARABOLIC EXPANSION OF CHI-SQUARED.
C
C     DESCRIPTION OF PARAMETERS
C
C     XD-ARRAY OF DATA POINTS FOR THE CURRENT
C     YD-ARRAY OF DATA POINTS FOR THE FINAL CONCENTRATION OF CH3I
C     S-ARRAY OF RADIALLY AVERAGED ENERGY-INTEGRATED CROSS-SECTIONS
C     SIGMAY-ARRAY OF STANDARD DEVIATIONS OF YD
C     NPTS-NUMBER OF PAIRS OF DATA POINTS
C     NTERMS-NUMBER OF FITTING PARAMETERS
C     MODE-DETERMINES METHOD OF WEIGHTING
C         +1-INSTRUMENTAL WEIGHTS
C          0-NO WEIGHTING
C         -1-STATISTICAL WEIGHTING
C     A-ARRAY OF FITTING PARAMETERS
C     DELTAA-ARRAY OF INCREMENTS FOR A
C     SIGMAA-ARRAY OF STINDARD DEVIATIONS FOR A
C     YFIT-ARRAY OF CALCULATED VALUES OF Y
C     CHISQR-REDUCED CHISQARE FOR FIT
C
C     SUBROUTINES AND FUNCION SUBPROGRAMS USED
C
C     STIFFZ
C             AELIB SUBROUTINE WHICH SOLVES SYSTEMS OF SIMULTANEOUS
C             DIFFERENTIOAL EQUATIONS.
C             (NOTE-THIS SUBROUTINE CALLS UP SEVERAL OTHERS AS
C             INDICATED IN AELIB MANUAL)
C     FCHISQ
C             EXTERNAL FUNCTION WHICH EVALUATES THE REDUCED CHI-
C             SQUARE FOR THE FIT TO THE DATA
C     SOLVEQN
C             INVERTS A SYMMETRIC TWO DIMENSIONAL MATRIX OF DEGREE
C             NTERMS AND CALCULATES ITS DETERMINANT
C     SOLV
C             INITIALIZES PARAMETERS FOR STIFFZ,AND CALLS UP STIFFZ
C             WHEN NECESSARY
C     EQNSF
C             CONTAINS THE SYSTEM OF DIFFERENTIAL EQUATIONS TO BE
```

```
C               SOLVED
C
C       COMMENTS
C
C       DIMENSION STATEMENT VALID FOR NTERMS UP TO 4.
C       PROGRAM IS SPECIFICALLY DESIGNED TO SOLVE THE DECOMPOSITION OF
C       METHYL IODIDE IN A NITROGEN CORONA DISCHARGE.
C
C       MORE PARAMETERS
C       A(1)-"RATE" OF HIGH EHERGY PROCESS
C       A(2)-RATE OF IODINE SPECIES DIFFUSING TO WALL
C       A(4)-MAXIMUM CROSS-SECTION FOR ELECTRON CAPTURE BY CH3I
C       A(3)-RATE OF REACTION BETWEEN METHYL RADICALS AND METHYL IODIDE
C       R1-RATE OF GAS-PHASE REACTION BETWEEN CH3 AND I(I2)
C       R2-RATE OF RECOMBINATION OF METHYL RADICALS
C       R3-RATE OF RECOMBINATION OF I ATOMS
C
C
        R1=241.3
        R2=1038.
        R3=7.239
        A(1)=0.005
        A(2)=5.0
        A(3)=5.0
        A(4)=200.
        A(5)=0.5
        DELTAA(1)=0.003
        DELTAA(2)=3.0
        DELTAA(4)=30.0
        DELTAA(3)=.3
        NTERMS=4
        MODE=0
        N=4
C
C       READ DATA FILE WITH FORMAT:
C
C       NPTS,FLO,N,YO
C       XD(I),S(I),YD(I)
C         "      "     "
C
        READ(5,1000) NPTS,FLO,N,YO
        READ(5,1100) (XD(I),S(I),YD(I),I=1,NPTS)
        DO 3 I=1,NPTS
    3   S(I)=S(I)/250
        WRITE(6,1300)
        WRITE(6,1000) NPTS,FLO,N,YO
        WRITE(6,1100) (XD(I),S(I),YD(I),I=1,NPTS)
        N=4
        DO 12 I=1,NPTS
   12   SIGMAY(I)=0.0
        NFREE=NPTS-NTERMS
        FREE=NFREE
        IF(NFREE) 14,14,199
   14   CHISQR=0.
        GO TO 150
C
C       COARSE SEARCH FIRST,FIND THE REGION OF MINIMUM CHI SQUARE
C
  199   DO 200 I=1,NPTS
        CURR=XD(I)
        CROSS=S(I)
        CALL SOLV(Y,T)
        YFIT(I)=Y(1)
```

```
 200    CONTINUE
        CHISQ1=FCHISQ(YD,SIGMAY,NPTS,NFREE,MODE,YFIT)
C
C       ITERATE PARAMETERS,TO FIND BEST ESTIMATE AB(I)
C
        DO 300 J=1,NTERMS
C
C       A(J)+DELTAA(J)
C
        AJ=A(J)
        A(J)=AJ+DELTAA(J)
        DO 215 I=1,NPTS
        CURR=XD(I)
        CROSS=S(I)
        CALL SOLV(Y,T)
        YFIT(I)=Y(1)
 215    CONTINUE
        CHISQ2=FCHISQ(YD,SIGMAY,NPTS,NFREE,MODE,YFIT)
        IF(CHISQ2.GE.CHISQ1) GO TO 225
        CHISQ1=CHISQ2
        DO 220 JJ=1,NTERMS
 220    AB(JJ)=A(JJ)
 225    DO 250 K=1,NTERMS
C
C       A(J)+DELTAA(J) AND A(K)+DELTAA(K)
C
        IF(K.LE.J) GO TO 250
        AK=A(K)
        A(K)=AK+DELTAA(K)
        DO 230 I=1,NPTS
        CURR=XD(I)
        CROSS=S(I)
        CALL SOLV(Y,T)
        YFIT(I)=Y(1)
 230    CONTINUE
        CHISQ3=FCHISQ(YD,SIGMAY,NPTS,NFREE,MODE,YFIT)
        A(K)=AK
        IF(CHISQ3.GE.CHISQ1) GO TO 250
        CHISQ1=CHISQ3
        DO 235 JJ=1,NTERMS
 235    AB(JJ)=A(JJ)
 250    CONTINUE
C
C       A(J)-DELTAA(J)
C
        A(J)=AJ-DELTAA(J)
        DO 245 I=1,NPTS
        CROSS=S(I)
        CURR=XD(I)
        CALL SOLV(Y,T)
        YFIT(I)=Y(1)
 245    CONTINUE
        CHISQ3=FCHISQ(YD,SIGMAY,NPTS,NFREE,MODE,YFIT)
        IF(CHISQ3.GE.CHISQ1) GO TO 260
        CHISQ1=CHISQ3
        DO 255 JJ=1,NTERMS
 255    AB(JJ)=A(JJ)
 260    A(J)=AJ
 300    CONTINUE
C
C       FINE SEARCH AND FIT USING PINITIAL PARAMETERS AS DETERMINED
C       BY COARSE FIT
C
```

```
      DO 270 JJ=1,NTERMS
      DELTAA(JJ)=0.1*AB(JJ)
270   A(JJ)=AB(JJ)
 16   DO 30 I=1,NPTS
      CURR=XD(I)
      CROSS=S(I)
      T=0.0
      CALL SOLV(Y,T)
      YFIT(I)=Y(1)
 30   CONTINUE
      CHISQ1=FCHISQ(YD,SIGMAY,NPTS,NFREE,MODE,YFIT)
      CHISQ4=CHISQ1
C
C     EVALUATE ALPHA AND BETA MATRICES
C
 20   DO 60 J=1,NTERMS
C
C     A(J)=A(J)+DELTAA(J)
C
 21   AJ=A(J)
      A(J)=AJ+DELTAA(J)
      DO 24 I=1,NPTS
      CURR=XD(I)
      CROSS=S(I)
      T=0.0
      CALL SOLV(Y,T)
      YFIT(I)=Y(1)
 24   CONTINUE
      CHISQ2=FCHISQ(YD,SIGMAY,NPTS,NFREE,MODE,YFIT)
      IF(1.05*CHISQ2.LT.CHISQ4) GO TO 16
      ALPHA(J,J)=CHISQ2-2*CHISQ1
      BETA(J)=-CHISQ2
 31   DO 50 K=1,NTERMS
      IF(K-J) 33,50,36
 33   ALPHA(K,J)=(ALPHA(K,J)-CHISQ2)/2.
      ALPHA(J,K)=ALPHA(K,J)
      GO TO 50
 36   ALPHA(J,K)=CHISQ1-CHISQ2
C
C     A(J)+DELTAA(J) AND A(K)+DELTAA(K)
C
 41   AK=A(K)
      A(K)=AK+DELTAA(K)
      DO 44 I=1,NPTS
      CURR=XD(I)
      CROSS=S(I)
      T=0.0
      CALL SOLV(Y,T)
      YFIT(I)=Y(1)
 44   CONTINUE
      CHISQ3=FCHISQ(YD,SIGMAY,NPTS,NFREE,MODE,YFIT)
      IF(1.05*CHISQ3.LT.CHISQ4) GO TO 16
      ALPHA(J,K)=ALPHA(J,K)+CHISQ3
      A(K)=AK
 50   CONTINUE
C
C     A(J)-DELTAA(J)
C
 51   A(J)=AJ-DELTAA(J)
      DO 53 I=1,NPTS
      CURR=XD(I)
      CROSS=S(I)
      T=0.0
```

```
      CALL SOLV(Y,T)
      YFIT(I)=Y(1)
 53   CONTINUE
      CHISQ3=FCHISQ(YD,SIGMAY,NPTS,NFREE,MODE,YFIT)
      IF(1.05*CHISQ3.LT.CHISQ4) GO TO 16
      A(J)=AJ
      ALPHA(J,J)=(ALPHA(J,J)+CHISQ3)/2.
      BETA(J)=(BETA(J)+CHISQ3)/4.
 60   CONTINUE
      WRITE(6,3900)
      DO 3950 I=1,NTERMS
3950  WRITE(6,4000) (ALPHA(I,J),J=1,NTERMS)
3900  FORMAT(* CURVATURE MATRIX BEFORE MANIPULATION*,/)
4000  FORMAT(* *,E10.3,3X,E10.3,3X,E10.3,3X,E10.3)
C
C     ELIMINATE NEGATIVE CURVATURE
C
 61   DO 70 J=1,NTERMS
      IF(ALPHA(J,J)) 63,65,70
 63   ALPHA(J,J)=-ALPHA(J,J)
      GO TO 66
 65   ALPHA(J,J)=0.01
 66   DO 69 K=1,NTERMS
      IF(K-J) 68,69,68
 68   ALPHA(J,K)=0.0
      ALPHA(K,J)=0.0
 69   CONTINUE
 70   CONTINUE
      WRITE(6,4100)
      DO 4150 I=1,NTERMS
4150  WRITE(6,4000) (ALPHA(I,J),J=1,NTERMS)
4100  FORMAT(* CURVATURE MATRIX AFTER MANIPULATION*,/)
C
C     INVERT MATRIX AND EVALUATE PARAMETER INCREMENTS
C
 71   CALL SOLVEQN(ALPHA,ALPH,NTERMS,NTERMS,MODE,NTERMS,NTERMS)
      WRITE(6,4200)
      DO 4250 I=1,NTERMS
4250  WRITE(6,4000) (ALPH(I,J),J=1,NTERMS)
4200  FORMAT(* CURVATURE MATRIX AFTER INVERSION*,/)
      DO 76 J=1,NTERMS
      DA(J)=0.
 74   DO 75 K=1,NTERMS
 75   DA(J)=DA(J)+BETA(K)*ALPH(J,K)
 76   DA(J)=0.2*DA(J)*DELTAA(J)
C
C     MAKE SURE CHISQUARE DECREASES
C
 81   DO 82 J=1,NTERMS
 82   A(J)=A(J)+DA(J)
 83   DO 84 I=1,NPTS
      CURR=XD(I)
      CROSS=S(I)
      CALL SOLV(Y,T)
      YFIT(I)=Y(1)
 84   CONTINUE
      CHISQ2=FCHISQ(YD,SIGMAY,NPTS,NFREE,MODE,YFIT)
      IF(CHISQ1-CHISQ2) 87,91,91
 87   DO 89 J=1,NTERMS
      DA(J)=DA(J)/2.
 89   A(J)=A(J)-DA(J)
      GO TO 83
C
```

```
C       INCREMENT PARAMETERS UNTIL CHISQUARED STARTS TO INCREASE
C
   91   DO 92 J=1,NTERMS
   92   A(J)=A(J)+DA(J)
        DO 94 I=1,NPTS
        CURR=XD(I)
        CROSS=S(I)
        T=0.0
        CALL SOLV(Y,T)
        YFIT(I)=Y(1)
   94   CONTINUE
        CHISQ3=FCHISQ(YD,SIGMAY,NPTS,NFREE,MODE,YFIT)
        IF(CHISQ3-CHISQ2) 97,100,101
   97   CHISQ1=CHISQ2
        CHISQ2=CHISQ3
   99   GO TO 91
C
C       FIND MINIMUM OF PARBOLA DEFINED BY LAST THREE POINTS
C
  100   DELTA=0.5
        GO TO 102
  101   DELTA=1./(1.+(CHISQ1-CHISQ2)/(CHISQ3-CHISQ2))+0.5
  102   DO 104 J=1,NTERMS
        ALPH(J,J)=ABS(ALPH(J,J))
        A(J)=A(J)-DELTA*DA(J)
  104   SIGMAA(J)=DELTAA(J)*SQRT(ALPH(J,J))
        DO 106 I=1,NPTS
        CURR=XD(I)
        CROSS=S(I)
        T=0.0
        CALL SOLV(Y,T)
        YFIT(I)=Y(1)
  106   CONTINUE
        CHISQR=FCHISQ(YD,SIGMAY,NPTS,NFREE,MODE,YFIT)
  111   IF(CHISQ2-CHISQR) 112,120,120
  112   DO 113 J=1,NTERMS
  113   A(J)=A(J)+(DELTA-1.)*DA(J)
        DO 115 I=1,NPTS
        CURR=XD(I)
        CROSS=S(I)
        T=0.0
        CALL SOLV(Y,T)
        YFIT(I)=Y(1)
  115   CONTINUE
        CHISQR=CHISQ2
  120   WRITE(6,1400)
        WRITE(6,1500) A(1),SIGMAA(1)
        WRITE(6,1600) A(2),SIGMAA(2)
        WRITE(6,1850) A(3),SIGMAA(3)
        WRITE(6,1800) A(4),SIGMAA(4)
        WRITE(6,1900)
        WRITE(6,2000)
        WRITE(6,2100)
        WRITE(6,2200) (XD(I),YD(I),YFIT(I),I=1,NPTS)
        WRITE(6,2300) CHISQR
C
C       FORMAT STATEMENTS
C
 1000   FORMAT(/,1X,I2,2X,F5.0,2X,I1,2X,F4.0,/)
 1100   FORMAT(1X,F5.2,3X,F7.5,3X,F6.2)
 1300   FORMAT(* INPUT DATA DECK*,/)
 1400   FORMAT(* PARAMETERS WHICH GAVE BEST FIT*,/)
 1500   FORMAT(* HIGH ENERGY INTEGRATED CROSS-SECTION=*,F6.4,* +/-*,
```

```
     1  F7.5)
 1600   FORMAT(* IODINE WALL REACTION RATE=*,F7.4,* +/-*,F8.5)
 1700   FORMAT(* METHYL WALL REACTION RATE=*,F7.4,* +/-*,F8.5)
 1800   FORMAT(* ELECTRON CAPTURE CROSS-SECTION=*,F5.0,* +/-*,F5.1)
 1850   FORMAT(* METHYL+METHYL IODIDE RATE=*,F7.4,* +/-*,F8.5,/)
 1900   FORMAT(* *,/,5X,* ###RESULTS###*,/)
 2000   FORMAT(* *,13X,* FINAL CONCENTRATIONS*)
 2100   FORMAT(* CURRENT*,5X,* DATA*,6X,* MODEL*,/)
 2200   FORMAT(* *,1X,F5.2,6X,F5.1,5X,F5.1)
 2300   FORMAT(* REDUCED CHI SQUARE=*,E10.3)
  150   STOP
        END
        SUBROUTINE SOLV(Y,T)
C
C       THIS SUBROUTINE CALLS UP STIFFZ TO SOLVE THE SYSTEM
C       OF DIFFERENTIAL EQUATIONS DEFINED IN EQNSF
C
        DIMENSION Y(4),WS(62),A(4)
        COMMON/STAT/KOUNT(7)
        COMMON/XTZQ/YO,FLO,A,CURR,CROSS,R1,R2,R3
        EXTERNAL EQNSF
C
C       INITIALIZE PARAMETERS
C
        T=0.0
        N=4
        Y(1)=YO
        DO 5 M=2,4
    5   Y(M)=0.0
        EPS=1.0E-08
        MF=22
        INOUT=0
        WS(1)=62.
        DTINT=31320.0/FLO
   10   CALL STIFFZ(EQNSF,Y,N,T,DTINT,EPS,H,MF,INOUT,WS)
        IF(INOUT.LT.-1) GO TO 50
        IF(T.LT.DTINT) GO TO 10
        GO TO 20
C
C       STOPS DUE TO ERROR
C
   50   WRITE(6,100) INOUT,KOUNT
  100   FORMAT(* INOUT=*,I3,* KOUNT=*,7I5)
   20   RETURN
        END
        SUBROUTINE EQNSF(N,T,Y,DY)
        REAL Y(N),DY(N),A(4)
        COMMON/XTZQ/YO,FLO,A,CURR,CROSS,R1,R2,R3
C
C       THESE EQUATIONS DEFINE THE REACTION SCHEME, WITH THE
C       SUBSTITUTIONS:
C       Y(1)=CH3I     Y(2)=CH3
C       Y(3)=I        Y(4)=I2
C       ALL CONCENTRATIONS IN UL/L
C
        DY(1)=(-A(3)*Y(1)+R1*(Y(3)+Y(4)))*Y(2)
     1  -0.4956*CURR*(A(1)*Y(1)+1-EXP(-Y(1)*A(4)*CROSS))
        DY(2)=0.4956*CURR*(A(1)*Y(1)+1-EXP(-Y(1)*A(4)*CROSS))-Y(2)*
     1  (R1*(Y(3)+Y(4))+A(3)*Y(1)+2.0*R2*Y(2))
        DY(3)=0.4956*CURR*(A(1)*Y(1))-2.0*R3*Y(3)**2-A(2)*Y(3)+R1*
     1  Y(2)*(Y(4)-Y(3))+A(3)*Y(1)*Y(2)
        DY(4)=R3*Y(3)**2-A(2)*Y(4)-R1*Y(2)*Y(4)
   10   RETURN
```

```
      END
C
C     FUNCTION FCHISQ
C
C     PURPOSE
C             EVALUATE REDUCED CHISQUARE  FOR  FIT TO DATA
C             FCHISQ=SUM((Y-YFIT)**2/SIGMA**2)/NFREE
C
      FUNCTION FCHISQ(Y,SIGMAY,NPTS,NFREE,MODE,YFIT)
      DIMENSION Y(1),SIGMAY(1),YFIT(1),A(4)
      COMMON/XTZQ/YO,FLO,A,CURR,CROSS,R1,R2,R3
      WRITE(6,800)
      WRITE(6,900) (A(I),I=1,5)
  800 FORMAT(* PARAMETERS*,/)
  900 FORMAT(* A(1)=*,E10.3,* A(2)=*,E10.3,* A(3)=*,E10.3,
     1* A(4)=*,E10.3,/)
      WRITE(6,1000)
      WRITE(6,1100) (Y(I),YFIT(I),I=1,NPTS)
 1000 FORMAT(* *,/,*    DATA*,4X,* FIT*)
 1100 FORMAT(* *,2X,F8.4,2X,F8.4)
   11 CHISQ=0.
   12 IF(NFREE) 13,13,20
   13 FCHISQ=0.
      GO TO 40
C
C     ACCUMULATE CHI SQUARE
C

   20 DO 30 I=1,NPTS
   21 IF(MODE) 22,27,29
   22 IF(Y(1)) 25,27,23
   23 WEIGHT=1/Y(I)
      GO TO 30
   25 WEIGHT=1/(-Y(I))
      GO TO 30
   27 WEIGHT=1.
      GO TO 30
   29 WEIGHT=1./SIGMAY(I)**2
   30 CHISQ=CHISQ+WEIGHT*(Y(I)-YFIT(I))**2
C
C     DIVIDE BY NUMBER OF DEGREES OF FREEDOM
C
      FREE=NFREE
      FCHISQ=CHISQ/FREE
      WRITE(6,2000) FCHISQ
 2000 FORMAT(* *,/,* FCHISQ=*,E14.7,/)
   40 RETURN
      END
C     THESE ARE ALL DUMMY SUBROUTINES
C
      SUBROUTINE DECB
      RETURN
      END
      SUBROUTINE SOLB
      RETURN
      END
      SUBROUTINE JAKOB
      RETURN
      END
      SUBROUTINE SPARSE
      RETURN
      END
      SUBROUTINE SPARSEB
```

```
      RETURN
      END
      SUBROUTINE SORTAG
      RETURN
      END
      SUBROUTINE MSCALE
      RETURN
      END
```